

ETH ZÜRICH

SEMESTER THESIS

**Search for Non-Interactive Entanglement  
Distillation Protocols Aided by Numerical  
Optimization**

*Author:*  
Yves SALATHÉ

*Advisor:*  
Dejan DUKARIC  
*Supervisor:*  
Prof. Dr. Stefan WOLF

March 21, 2011

## Abstract

Entanglement is a property of physical reality that cannot be explained by the classical laws of physics [1]. In quantum cryptography, entangled pairs of photons are used to establish secure channels and in quantum computing entanglement is a resource that can be used to send the state of a qubit from one location to another [2] using classical communication. An important question in the context of physical realizations of entangled systems is whether entanglement can be restored from the imperfectly entangled systems resulting from decoherence. The Schmidt projection method by Bennet et. al. [3] can concentrate entanglement from many copies of an entangled pure state into a smaller set of perfectly entangled states. Unlike many protocols that were later developed for mixed states [4, 5, 6, 7, 8], the Schmidt projection method works without communication. On the other hand, the Schmidt projection method only becomes efficient if a large number of copies of the initially entangled state are given. In the first part of this work we show that the Schmidt projection method cannot be used to increase the fully entangled fraction if used with only two copies of an entangled pure input state and under the assumption that no post selection is allowed. Conversely, we show that this task is possible if one has 3 copies of a pure input pair instead. From the protocol for 3 copies of a pure state, we derive a non-interactive protocol that works for certain mixed states. In the second part we demonstrate the possibility to numerically find entanglement distillation protocols that do not use communication by solving a high dimensional optimization problem using the evolutionary algorithm CMA-ES [9].

# Contents

<b>Contents</b>	<b>1</b>
<b>1 Introduction</b>	<b>2</b>
<b>2 Foundations</b>	<b>4</b>
2.1 The Qubit . . . . .	4
2.2 Many Qubits: Combined Systems . . . . .	5
2.3 Measurements, Mixed States and the Partial Trace . . . . .	6
2.4 Entanglement . . . . .	7
<b>3 Entanglement Measures</b>	<b>10</b>
3.1 Local Operations and Classical Communication . . . . .	10
3.2 Entropy of Entanglement . . . . .	10
3.3 Fidelity and the Fully Entangled Fraction . . . . .	11
<b>4 Entanglement Distillation Protocols</b>	<b>14</b>
4.1 Single Pair Purification . . . . .	14
4.2 Protocols without communication . . . . .	15
4.3 General Limitations and Optimality . . . . .	15
4.4 A Note On The Schmidt Projection Method For Two Copies . . . . .	16
<b>5 Numerical Optimization</b>	<b>19</b>
5.1 Parameterization of Unitary Matrices . . . . .	20
5.2 Black-Box Optimization With CMA-ES . . . . .	21
5.3 Results for 3 copies of a pure initial state with 2 ancilla qubits per party	22
5.3.1 Optimization over a Single Orthogonal Matrix . . . . .	22
5.3.2 Unrestricted Optimization over 2 Unitary Matrices . . . . .	24
5.4 Results for 2 copies of a pure initial state . . . . .	27
5.5 Results for 3 copies of a Werner state . . . . .	27
<b>6 Conclusions</b>	<b>31</b>
<b>A Proof of Theorem 4.3.1</b>	<b>33</b>
<b>B Proof of Theorem 4.4.1</b>	<b>35</b>
<b>C Tables</b>	<b>38</b>
C.1 Entanglement Distillation Protocols . . . . .	38
C.2 Limits to Distillability . . . . .	40
C.3 Optimization Runs . . . . .	42
<b>Bibliography</b>	<b>47</b>

# Chapter 1

## Introduction

The field of quantum information theory deals with the implications of quantum mechanics on our ability to process information and vice-versa combines the known theoretical results from information theory and related fields with quantum theory to make predictions about the behaviour of nature. One of the most surprising features of quantum mechanics is entanglement. In 1935, Einstein et. al. [10] argued that the so called “reduction of the wave packet”, i.e. the way measurements are described in quantum mechanics leads to a paradoxical situation where the probabilities of different results of a measurement that is performed on one of two or more spatially separated systems will affect the state of the combined system even though the systems are not able to interact by means of any known physical interaction. They conclude that quantum mechanics is thus unlikely to describe nature in a complete way. In 1964, John Bell [1] found a way to test whether such instantaneous effects exist in nature by formulating an inequality that limits the correlations of simultaneous local measurements on two subsystems under the assumption that the subsystems cannot interact during the time the measurements are performed. John Bell predicted that if nature acts quantum mechanically, his inequality will be violated by so called entangled states. Aspect et. al. verified the violation of the Bell inequalities by experiment. To our present knowledge exactly the opposite of Einstein’s conclusion is true: we need quantum mechanics to describe effects like entanglement. Since then, a lot of research has dealt with the question whether we can use entanglement to perform useful tasks. In 1984, Bennet and Brassard [11] proposed a secure way to exchange one time pads for encrypted communication. In 1992 Bennet and Wiesner [3] showed that it is possible to send two classical bits by sending a so called qubit (a quantum mechanical two-state system), if the sender (Alice) and the receiver (Bob) initially share an entangled pair of qubits. In 1993, Bennet et. al. [2] developed a quantum protocol that uses an entangled pair of qubits to send the state of a quantum bit from one location to another by sending two classical bits. In fact, entanglement has become a resource to perform different tasks that would be impossible without it.

However, a major problem with physical implementations of these ideas is that the systems cannot be perfectly isolated. The system interacts with the environment in a way that cannot be perfectly predicted and controlled. This so called decoherence can destroy entanglement or make it weaker. So we need a way to restore it. This is where entanglement distillation comes into play. Bennet et. al. [12] were the first to develop two protocols that can concentrate entanglement from many copies of imperfectly entangled pairs of qubits into a smaller set of perfectly entangled qubits. One of the two protocols (called Schmidt projection) has the surprising property that it can be executed without the need of communication between the two distinct subsystems. While

the Schmidt projection protocol was shown to be asymptotically optimal [13], there are two drawbacks: it only works for a large number of copies and only for pure states. The effect of decoherence is that the state of the system is transformed into a mixture of different states. To account for this kind of randomness, different protocols were found in various preceding publications that all deal with a certain type of mixed state [4, 5, 6, 7, 8]. Previous research on limits to the existence of non-interactive protocols for mixed states [7, 8, 14, 15] has revealed that there are many states for which entanglement distillation without communication is not possible. In the present work we further investigate the possibility of entanglement distillation without communication by summarizing the known results about the existence and non-existence of protocols in Chapter 4 and proving that the Schmidt projection method does not work without post-selection if only two copies of an imperfectly entangled state are given. In the second part of the work (Chapter 5) we demonstrate the possibility to find entanglement protocols by numerical optimization. Chapter 2 and 3 provide the foundations to introduce the notation and definitions needed to state the results of the present work.

# Chapter 2

## Foundations

The purpose of this chapter is to give an overview of the notation and concepts that are used in the present work.

### 2.1 The Qubit

The basic element of quantum information science, the quantum bit (qubit), is a physical system that acts quantum mechanical and has two distinguishable states. For such systems, the postulates of quantum mechanics (see e.g. [16, 17, 18]) imply that its state is described by a wave function, allowing it to be in any superposition of two basis states. One usually writes the state of the Qubit in Dirac's Ket notation:  $|\psi\rangle \in \mathcal{H}_2$ , where  $\mathcal{H}_2$  is the two-dimensional Hilbert space, which means that the state is represented by a complex-valued two-dimensional vector. One defines the two vectors

$$|0\rangle = \begin{pmatrix} 1 \\ 0 \end{pmatrix}, \quad |1\rangle = \begin{pmatrix} 0 \\ 1 \end{pmatrix}. \quad (2.1)$$

The set  $\{|0\rangle, |1\rangle\}$  is called "computational basis". An arbitrary one-qubit pure state can then be written as:

$$|\psi\rangle = \begin{pmatrix} \alpha \\ \beta \end{pmatrix} = \alpha|0\rangle + \beta|1\rangle, \quad (2.2)$$

where  $\alpha, \beta \in \mathbb{C}^2$  and the states  $|0\rangle$  and  $|1\rangle$  are orthogonal i.e.  $\langle 0|1\rangle = \langle 1|0\rangle = 0$ . Note that the flipped Ket denotes the conjugate transpose of the corresponding vector, i.e.  $\langle \psi| = (|\psi\rangle)^\dagger$  and is called "Bra".

Since the qubit is quantum mechanical, its time-evolution is described by the time-dependent Schrödinger equation

$$i\hbar \frac{\partial}{\partial t} |\psi(t)\rangle = \hat{H}(t) |\psi(t)\rangle, \quad (2.3)$$

where  $\hat{H}(t)$  is the Hamiltonian operator and  $\hbar$  is Planks constant (see e.g. [19] for its physical value). The general solution of this equation can be written as

$$|\psi(t)\rangle = e^{-\frac{i}{\hbar} \int_0^t \hat{H}(\tilde{t}) d\tilde{t}} |\psi(0)\rangle. \quad (2.4)$$

This can be verified by inserting (2.4) into (2.3). Since the Hamiltonian operator  $\hat{H}$  is hermitean, the linear operator  $\hat{T} := \exp(-\frac{i}{\hbar} \int_0^t \hat{H}(\tilde{t}) d\tilde{t})$  on the right hand side of Equation (2.4) is unitary:

$$\hat{T}^\dagger \hat{T} = \hat{T} \hat{T}^\dagger = e^{-\frac{i}{\hbar} \int_0^t \hat{H}(\tilde{t}) d\tilde{t}} e^{+\frac{i}{\hbar} \int_0^t \hat{H}(\tilde{t}) d\tilde{t}} = e^{\frac{i}{\hbar} (\int_0^t \hat{H}(\tilde{t}) d\tilde{t} - \int_0^t \hat{H}(\tilde{t}) d\tilde{t})} = e = \mathbf{1}. \quad (2.5)$$

Operations on qubits are therefore represented by unitary matrices.

The above statement leads to the so called quantum parallelism, which comes from the fact that the unitary operation  $\mathbf{U}$  is linear. Thus, if it is applied on a state given by Equation (2.2) one gets

$$\mathbf{U}|\psi\rangle = \mathbf{U}(\alpha|0\rangle + \beta|1\rangle) = \alpha\mathbf{U}|0\rangle + \beta\mathbf{U}|1\rangle, \quad (2.6)$$

so the unitary operation acts on both basis states in the superposition simultaneously! This is one of the reasons why quantum algorithms can have lower complexity than the corresponding classical algorithms. Conversely, it is not so easy to design algorithms that outperform their classical counterparts since the state vector cannot be completely determined with a single measurement and because the measurement itself modifies the state vector, as will be detailed in Section 2.3.

## 2.2 Many Qubits: Combined Systems

To see how a system of two or more qubits can be composed from the ones of single qubits, it is best to think about how one would combine two classical bits. Such a classical combined system of two bits is described by the states of the individual bits. Since every classical bit can take on the values 0 or 1 (two possible characters), there are four possible states for the combined system: 00 01 10 and 11 (string over an alphabet of two characters). As seen in Section 2.1, this stands in contrast to quantum systems, where each qubit is described by a two-dimensional complex-valued vector, the components of which having the meaning of complex probability amplitudes for the event that the systems are in their respective two distinct basis states (usually denoted as  $|0\rangle$  and  $|1\rangle$ ). As for the classical combined system, a two qubit system is defined such that it has four different basis states  $|00\rangle$ ,  $|01\rangle$ ,  $|10\rangle$  and  $|11\rangle$ . The difference lies in the postulate that such a quantum system has to be described by a *four*-dimensional vector, each component describing the probability amplitude for the corresponding basis state. In fact, the state of the combined system is contained in the tensor product of the Hilbert spaces  $\mathcal{H}_A$  and  $\mathcal{H}_B$  of the individual subsystems:

$$\mathcal{H}_{AB} = \mathcal{H}_A \otimes \mathcal{H}_B, \quad (2.7)$$

where the basis vectors that span  $\mathcal{H}_{AB}$  are the four different tensor products of the basis states of the single qubit systems, i.e.

$$|00\rangle = |0\rangle \otimes |0\rangle, \quad (2.8)$$

$$|01\rangle = |0\rangle \otimes |1\rangle, \quad (2.9)$$

$$|10\rangle = |1\rangle \otimes |0\rangle, \quad (2.10)$$

$$|11\rangle = |1\rangle \otimes |1\rangle. \quad (2.11)$$

$$(2.12)$$

An arbitrary state  $|\psi\rangle$  of the combined system is then written in terms of these basis states, i.e.

$$|\psi\rangle = \alpha|00\rangle + \beta|01\rangle + \gamma|10\rangle + \delta|11\rangle, \quad (2.13)$$

with complex coefficients  $\alpha, \beta, \gamma, \delta \in \mathbb{C}$ .

This has wide ranging consequences: While each individual qubit, if in a pure state, has 3 degrees of freedom (the real and imaginary parts of the two coefficients  $\alpha$  and  $\beta$  in (2.2) minus one degree of freedom due to the normalization constraint),

the pure state of the combined system has 7 degrees of freedom (again the real and imaginary parts of the four coefficients  $\alpha, \beta, \gamma$  and  $\delta$  minus one degree of freedom due to the normalization constraint). So the combined system has actually more degrees of freedom than just the sum of the degrees of freedom of the individual systems! This already indicates that there are states of the combined system, that cannot be represented by just combining the vectors that describe the states of the individual system. In Section 2.4, particular examples of such states will be presented. Another important consequence can be seen from the way the number of basis states increases: For a system of  $n$  qubits, the states that form a complete basis set can be labelled by all possible  $n$ -bit-strings, of which there are exactly  $2^n$ . So the cardinality of the complete set of basis states, and hence the dimensionality, grows exponentially! This indicates how hard it is to simulate a large-scale quantum system on a classical computer.

### 2.3 Measurements, Mixed States and the Partial Trace

In quantum mechanics, a measurement is described by a set of operators  $\{\mathbf{M}_i \mid i = 1, \dots, n\}$  that map the pre-measurement state to the post-measurement state that corresponds to a particular measurement result. Before a certain quantity is measured, it may in fact not yet be determined for a certain state. Mathematically, the probability to measure the result corresponding to  $\mathbf{M}_i$  if the system is in a pure state  $|\psi\rangle$  is

$$p_i := \langle \psi | \mathbf{M}_i | \psi \rangle \quad (2.14)$$

. The state  $|\phi\rangle$  after the measurement will be

$$|\phi_i\rangle = \frac{\mathbf{M}_i |\psi\rangle}{\sqrt{p_i}}, \quad (2.15)$$

when the measurement result is known to correspond to  $\mathbf{M}_i$  for a certain index  $i$ . If the measurement operators  $\mathbf{M}_i$  are projection operators, the corresponding measurement is called projective measurement.

Related to the concept of measurements is the density operator. It is used to describe classical uncertainty in quantum mechanics. E.g. if one knows a certain measurement has been performed on a system that was in a known state before it was measured but one does not know the measurement result. In that case, one still knows the probability  $p_i$  with which each measurement result is obtained i.e. the probability  $p_i$  that the system is in a certain pure post-measurement state  $|\phi_i\rangle$ . This situation, which is called a mixed state, is described by the density operator

$$\rho = \sum_i p_i |\phi_i\rangle \langle \phi_i|. \quad (2.16)$$

Density operators are positive operators i.e.  $\rho^\dagger = \rho$  and the eigenvalues are real-valued and non-negative. Furthermore the trace (the sum of diagonal elements which is equal to the sum of eigenvalues) of density operators is defined to be one, i.e.  $\text{tr}(\rho) = 1$ . Note that for a system in a pure state  $|\psi\rangle$ , the density operator  $\rho$  corresponding to that state is the outer product of  $|\psi\rangle$  with itself:  $\rho = |\psi\rangle \langle \psi|$ .

If a measurement is performed on a system in a state described by the density operator  $\rho$ , then the probabilities of the measurement outcomes are determined by

$$p_i = \text{tr}(\mathbf{M}_i \rho). \quad (2.17)$$

The post-measurement state will be determined by

$$\rho_i = \frac{\mathbf{M}_i \rho \mathbf{M}_i^\dagger}{p_i}. \quad (2.18)$$



Another reason for having a mixed state may be that the system in concern interacts with another system (e.g. the environment), but the state vector for the combined system is unknown. Suppose the state vector of the combined system of two subsystems  $A$  and  $B$  is  $|\psi\rangle$ , then the density operator  $\rho$  of a particular subsystem  $A$  will be determined by the so called partial trace over the subsystem  $B$

$$\rho_A = \text{tr}_B(|\psi\rangle\langle\psi|). \quad (2.19)$$

The partial trace  $\text{tr}_B(\rho)$  is computed by writing the density operator  $\rho$  in a basis where the basis vectors are separable, i.e.  $\{|\psi_i\rangle \mid |\psi_i\rangle = |\psi_{A,k}\rangle \otimes |\psi_{B,l}\rangle, i = 1, \dots, d\}$ , where  $|\psi_{A,k}\rangle$  is a state vector of subsystem  $A$  and  $|\psi_{B,l}\rangle$  one of subsystem  $B$ :

$$\rho = \sum_i \sum_j \sum_k \sum_l \alpha_{i,j} (|\psi_{A,i}\rangle\langle\psi_{A,k}| \otimes (|\psi_{B,j}\rangle\langle\psi_{B,l}|)), \quad (2.20)$$

Then the partial trace  $\text{tr}_B(\rho)$  is

$$\rho_{BP} = \sum_i \sum_j \sum_k \sum_l \alpha_{i,j} (|\psi_{A,i}\rangle\langle\psi_{A,k}| \text{tr}(|\psi_{B,j}\rangle\langle\psi_{B,l}|)) \quad (2.21)$$

$$= \sum_i \sum_k \alpha_{i,j} \left( |\psi_{A,i}\rangle\langle\psi_{A,k}| \sum_j \sum_l \langle\psi_{B,j}|\psi_{B,l}\rangle \right). \quad (2.22)$$

## 2.4 Entanglement

As already mentioned in Section 2.2, there are quantum mechanical systems for which the state of the system as a whole is not completely determined by the states of the individual subsystems. Take for example a system that consists of two subsystems. Let us consider the following state of the combined system

$$|\psi^+\rangle = \frac{1}{\sqrt{2}}(|00\rangle + |11\rangle). \quad (2.23)$$

There is no way to write  $|\psi^+\rangle$  as a tensor product of the states of subsystems  $A$  and  $B$ , i.e.

$$|\psi^+\rangle \neq |\psi_A\rangle \otimes |\psi_B\rangle. \quad (2.24)$$

A state that has this property is called a non-separable or entangled state.

Now imagine that the two subsystems are spatially separated, i.e. one qubit is at Alice's location and the other qubit is at Bob's location but the state of the system that includes both qubits is still described by Equation (2.23). A consequence of the system being in the state  $|\psi^+\rangle$  is that if the qubits are measured locally, i.e. if Alice measures the system with the set of operators  $\{|0\rangle\langle 0| \otimes \mathbb{1}, |1\rangle\langle 1| \otimes \mathbb{1}\}$  and Bob uses the operators  $\{\mathbb{1} \otimes |0\rangle\langle 0|, \mathbb{1} \otimes |1\rangle\langle 1|\}$ , they will get the same measurement result with certainty, given that they choose the same measurement basis. Although Alice and Bob measure the same value, the outcome of their measurement will be random. To see this, we use the knowledge of 2.3 and calculate the probabilities  $p_0$  and  $p_1$  using Formula (2.14) as well as the corresponding post-measurement states  $|\phi_0\rangle$  and  $|\phi_1\rangle$  using Formula (2.15) with e.g. Alice's set of measurement operators  $\{|0\rangle\langle 0| \otimes \mathbb{1}, |1\rangle\langle 1| \otimes \mathbb{1}\}$ .

If Alice and Bob choose two different sets of measurement operators to measure the state  $|\psi^+\rangle$  described by Equation (2.23), they will get the same result only with a certain probability.

Let Alice and Bob be far away from each other and let them perform the measurements on the state (2.23) within a small enough time window, so that their qubits cannot communicate through any known physical interaction. By the theory of relativity interaction cannot happen faster than the time it takes for a photon to travel in vacuum from Alice to Bob. Assume furthermore that Alice and Bob repeat the experiment with different measurement bases rotated to each other with different angles. One can show that the results of the measurement performed in this way violate the so called Bell inequality [1] which gives a bound for the value of a special correlation function under the assumption that the measurement results of Alice and Bob were predetermined by so called “hidden variables” which can only influence each other through the way of physical interaction (i.e. communication). So either the theory of quantum mechanics has to be considered wrong or the assumptions that were made to derive the Bell inequality do not conform with reality. The first experiment that was able to verify the violation of Bell’s inequality while excluding the possibility of communication between the subsystems of Alice and Bob during the time of the measurement was performed in 1982 by Aspect et. al. [20] with polarization-entangled photons. Since then, many experiments with different physical realizations of entanglement have shown that Bell’s inequality are violated in nature. Thus, nature behaves in a non-local and/or non-predetermined manner.

The above described setting, where there are qubits at two different locations, is called bipartite system. Not every state of the bipartite system can be used to violate the Bell inequalities. For example any separable state, i.e. a state that can be written as a tensor product of the states of the individual subsystems cannot be used to violate the Bell inequality. Those states that maximally violate the Bell inequality are called Bell or maximally entangled states and have the form

$$|\psi^+\rangle = \frac{1}{\sqrt{2}}(|0+\rangle + |1-\rangle), \quad (2.25)$$

$$|\psi^-\rangle = \frac{1}{\sqrt{2}}(|0+\rangle - |1-\rangle), \quad (2.26)$$

$$|\phi^+\rangle = \frac{1}{\sqrt{2}}(|0-\rangle + |0+\rangle), \quad (2.27)$$

$$|\phi^-\rangle = \frac{1}{\sqrt{2}}(|0-\rangle - |1+\rangle). \quad (2.28)$$

We denote the basis states of Alice’s subsystem as  $|0\rangle$  and  $|1\rangle$  and those of Bob  $|+\rangle$  and  $|-\rangle$  to make clear which qubits are at which location.

Despite of the violation of the Bell inequalities being a behaviour that cannot be explained by classical physics, entangled states cannot be used to communicate. This is indicated by the description of the subsystems by the partial trace of the combined system. The partial trace describes the absence of knowledge about the other subsystem. Let the combined system be in the state  $|\psi^+\rangle$ . Thus, the density operator is

$$\rho = |\psi^+\rangle\langle\psi^+| \quad (2.29)$$

$$= \frac{1}{2}(|00\rangle\langle 00| + |00\rangle\langle 11| + |11\rangle\langle 00| + |11\rangle\langle 11|) \quad (2.30)$$

$$= \frac{1}{2}(|0\rangle\langle 0| \otimes |0\rangle\langle 0| + |0\rangle\langle 1| \otimes |0\rangle\langle 1| + |1\rangle\langle 0| \otimes |1\rangle\langle 0| + |1\rangle\langle 1| \otimes |1\rangle\langle 1|). \quad (2.31)$$

If we now trace out the subsystem of e.g. Bob to get the state of the subsystem of

Alice, we get

$$\rho_A = \text{tr}_B(\rho) \tag{2.32}$$

$$= \frac{1}{2} \left( |0\rangle\langle 0| \underbrace{\langle 0|0\rangle}_1 + |0\rangle\langle 1| \underbrace{\langle 0|1\rangle}_0 + |1\rangle\langle 0| \underbrace{\langle 1|0\rangle}_0 + |1\rangle\langle 1| \underbrace{\langle 1|1\rangle}_1 \right) \tag{2.33}$$

$$= \frac{1}{2} (|0\rangle\langle 0| + |1\rangle\langle 1|) \tag{2.34}$$

$$= \frac{1}{2} \mathbb{1}. \tag{2.35}$$

So the state  $\rho_A$  is a mixed state where the probability that the system is in state  $|0\rangle$  is exactly  $\frac{1}{2}$ . No measurement on this state can reveal any information about Bob's subsystem.

## Chapter 3

# Entanglement Measures

### 3.1 Local Operations and Classical Communication

Since most applications of entanglement involve local operations and classical communication (LOCC) it may make sense to assume that those operations are freely available when the question of whether one state is more entangled than the other is addressed. For example one could ask whether the (pure) state  $|\psi_1\rangle$  can be turned into  $|\psi_2\rangle$  with only LOCC. If it is possible, the state  $|\psi_1\rangle$  is considered to have the same or more entanglement than  $|\psi_2\rangle$  since it is at least as useful as  $|\psi_2\rangle$  for any application.

In the present work, classical communication is usually not regarded as free and it would thus be more appropriate to exclude the ability to communicate in the definition of an entanglement measure. Nevertheless, we use the standard notion of entanglement in the present work, so that the results of this work can be compared directly to previously known results in the field of entanglement distillation research.

### 3.2 Entropy of Entanglement

For bipartite pure states  $|\psi\rangle$  one often uses the so called entropy of entanglement denoted as  $E(|\psi\rangle)$  as a measure. It is defined as the Von Neumann entropy  $S(\rho_{\psi,A})$  (see e.g. [18, p. 510]) of the density operator that describes one of the subsystems, e.g. Alice's:

$$\rho_{\psi,A} := \text{tr}_B |\psi\rangle\langle\psi|, \quad (3.1)$$

so that

$$E(|\psi\rangle) := S(\rho_{\psi,A}) = -\rho_{\psi,A} \log_2 \rho_{\psi,A}. \quad (3.2)$$

To compute  $E$ , one first computes the vector of eigenvalues  $\lambda$  of the density matrix  $\rho_{\psi,A}$  and then uses

$$E(|\psi\rangle) = S(\rho_{\psi,A}) = H(\lambda) := -\sum_i^d \lambda_i \log_2 \lambda_i, \quad (3.3)$$

where  $d$  is the dimension of the Hilbert space describing Alice's subsystem. The entropy of entanglement cannot be increased by LOCC as can be seen from the discussion in Section 4.3.

### 3.3 Fidelity and the Fully Entangled Fraction

The term fidelity is used for the probability for a state described by the density operator  $\rho$  to yield a pure state  $|\psi_{\text{ref}}\rangle$  when the corresponding system is measured with a set of operators that project on orthogonal subspaces containing the operator  $|\psi_{\text{ref}}\rangle\langle\psi_{\text{ref}}|$ . According to Formula (2.17), this probability is

$$\varphi_{|\psi_{\text{ref}}\rangle}(\rho) := \text{tr}(|\psi_{\text{ref}}\rangle\langle\psi_{\text{ref}}|\rho) = \langle\psi_{\text{ref}}|\rho|\psi_{\text{ref}}\rangle. \quad (3.4)$$

In the present work, the symbol  $\varphi_{|\psi_{\text{ref}}\rangle}(\rho)$  is used to denote the fidelity of state  $\rho$  with respect to the reference state  $|\psi_{\text{ref}}\rangle$ . If the subscript of  $\varphi$  is omitted, the fidelity with respect to the Bell state  $|\psi^+\rangle$  is meant.

The fully entangled fraction  $F(\rho)$  [5] is defined to be the maximal fidelity with respect to a maximally entangled state that one can get if local unitary operations are allowed to be performed before the (hypothetical) measurement. This entanglement measure is known to be well suited for the distinction of separable states from entangled states [21] and is very useful in the context of optimization of entanglement distillation protocols as will become clear in Chapter 5. Moreover, the fully entangled fraction is related to protocols that use a Bell state as a resource so that the fully entangled fractions determines the best achievable error rate of the quantum algorithm. Mathematically, the definition of the fully entangled fraction is

**Definition 3.3.1.** *The following equation defines the fully entangled fraction  $F(\cdot)$  of a state described by the density operator  $\rho$  of a bipartite two-qubit system represented by the four-dimensional Hilbert space  $\mathcal{H}_A \otimes \mathcal{H}_B$ , where  $\mathcal{H}_A$  and  $\mathcal{H}_B$  are two-dimensional Hilbert spaces.*

$$F(\rho) = \max_{|\phi\rangle:m.e.} \langle\phi|\rho|\phi\rangle, \quad (3.5)$$

where  $|\phi\rangle$  denotes any maximally entangled state.

For bipartite systems, Definition 3.3.1 can also be written in terms of unitary operations as follows

$$F(\rho) = \max_{U_A, U_B} \langle\phi^+|(U_A \otimes U_B)\rho(U_A^\dagger \otimes U_B^\dagger)|\phi^+\rangle, \quad (3.6)$$

where  $U_A$  and  $U_B$  denote arbitrary unitary operations on the Hilbert spaces  $\mathcal{H}_A$  and  $\mathcal{H}_B$  respectively and  $|\phi^+\rangle = \frac{1}{\sqrt{2}}(|0+\rangle + |1-\rangle)$ . This equivalence holds because in the bipartite case, the maximally entangled states are the Bell states (Section 2.4), which form a complete basis set and can be interconverted to each other by local unitary operations without communication [5].

Also notice that if the system is in a pure state, i.e.  $\rho = |\psi\rangle\langle\psi|$ , then the fully entangled fraction is simply

$$F(\rho) = \max_{U_A, U_B} |\langle\phi^+|(U_A \otimes U_B)|\psi\rangle|^2. \quad (3.7)$$

In the following, we will derive some properties of the fully entangled fraction that will be used in Chapter 4 in the context of the Schmidt projection method.

**Lemma 3.3.1.** *Let  $\rho = \sum_i c_i \rho_i$  be a linear combination of density matrices  $\rho_i$  with  $c_i \in [0, 1] \subseteq \mathbb{R}$ , then:*

$$F(\rho) \leq \sum_i c_i F(\rho_i), \quad (3.8)$$

where  $F(\rho)$  is the fully entangled fraction (Definition 3.3.1).

*Proof.*

$$F(\rho) = \max_{|\phi\rangle: \text{m.e.}} \langle \phi | (\sum_i c_i \rho_i) | \phi \rangle \quad (3.9)$$

$$= \max_{|\phi\rangle: \text{m.e.}} \sum_i c_i \langle \phi | \rho_i | \phi \rangle \quad (3.10)$$

$$\leq \sum_i c_i \max_{|\phi\rangle: \text{m.e.}} \langle \phi | \rho_i | \phi \rangle \quad (3.11)$$

The last equality holds because the coefficients  $c_i$  are non-negative and since an increase in the value of any sum over real numbers implies an increase in at least one term over which the sum is taken.  $\square$

Note that Theorem 1 in [22] gives a condition under which Equation 3.8 holds with equality, given that the sum on the right hand side is a convex combination of pure states.

**Lemma 3.3.2.** *Let  $\mathcal{H}_A$  and  $\mathcal{H}_B$  be two-dimensional Hilbert spaces and let  $|\psi\rangle$  be a separable pure state of the combined system, i.e.  $\rho := |\psi\rangle\langle\psi|$  with  $|\psi\rangle := |\psi_A\rangle \otimes |\psi_B\rangle$  for some states  $|\psi_A\rangle \in \mathcal{H}_A$  and  $|\psi_B\rangle \in \mathcal{H}_B$ . Then, the fully entangled fraction of the state  $\psi$  of the combined system is always less than or equal to 0.5.*

*Proof.* The pure states can be written in general as  $|\psi_A\rangle := \alpha_A|0\rangle + \beta_A|1\rangle$  and  $|\psi_B\rangle := \alpha_B|+\rangle + \beta_B|-\rangle$  for some complex coefficients  $\alpha_A, \alpha_B, \beta_A, \beta_B \in \mathbb{C}$  with  $|\alpha_A|^2 + |\beta_A|^2 = 1$  and  $|\alpha_B|^2 + |\beta_B|^2 = 1$ .

If any unitary operation of the form  $U_A \otimes U_B$  is applied on a tensor product state of the form  $|\psi_A\rangle \otimes |\psi_B\rangle$ , the state of the combined system can still be written as a tensor product:

$$(U_A \otimes U_B)(|\psi_A\rangle \otimes |\psi_B\rangle) = (U_A|\psi_A\rangle \otimes U_B|\psi_B\rangle) = (|\tilde{\psi}_A\rangle \otimes |\tilde{\psi}_B\rangle). \quad (3.12)$$

with  $|\tilde{\psi}_A\rangle := U_A|\psi_A\rangle = \tilde{\alpha}_A|0\rangle + \tilde{\beta}_A|1\rangle$  and  $|\tilde{\psi}_B\rangle := U_B|\psi_B\rangle = \tilde{\alpha}_B|+\rangle + \tilde{\beta}_B|-\rangle$ .

With the above definitions, the state of the combined system after application of any local unitary operations is

$$|\tilde{\psi}_A\rangle \otimes |\tilde{\psi}_B\rangle = \tilde{\alpha}_A \tilde{\alpha}_B |0+\rangle + \tilde{\alpha}_A \tilde{\beta}_B |0-\rangle + \tilde{\beta}_A \tilde{\alpha}_B |1+\rangle + \tilde{\beta}_A \tilde{\beta}_B |1-\rangle \quad (3.13)$$

Therefore we have

$$|\langle \phi^+ | (|\tilde{\psi}_A\rangle \otimes |\tilde{\psi}_B\rangle) \rangle|^2 = \left| \left( \frac{1}{\sqrt{2}} (\langle 0+ | + \langle 1- |) \right) (|\tilde{\psi}_A\rangle \otimes |\tilde{\psi}_B\rangle) \right|^2 \quad (3.14)$$

$$= \frac{1}{2} |\tilde{\alpha}_A \tilde{\alpha}_B + \tilde{\beta}_A \tilde{\beta}_B|^2 \quad (3.15)$$

$$\leq \frac{1}{2} (|\tilde{\alpha}_A \tilde{\alpha}_B|^2 + |\tilde{\beta}_A \tilde{\beta}_B|^2) \quad \text{subadditivity} \quad (3.16)$$

$$= \frac{1}{2} (|\tilde{\alpha}_A \tilde{\alpha}_B|^2 + (1 - |\tilde{\alpha}_A|^2)(1 - |\tilde{\alpha}_B|^2)) \quad (3.17)$$

$$= \frac{1}{2} (2|\tilde{\alpha}_A \tilde{\alpha}_B|^2 - |\tilde{\alpha}_A|^2 - |\tilde{\alpha}_B|^2 + 1) \quad (3.18)$$

$$= \frac{1}{2} \underbrace{\left( \underbrace{|\tilde{\alpha}_A|^2}_{\geq 0} (\underbrace{|\tilde{\alpha}_B|^2 - 1}_{\leq 0}) + \underbrace{|\tilde{\alpha}_B|^2}_{\geq 0} (\underbrace{|\tilde{\alpha}_A|^2 - 1}_{\leq 0}) + 1 \right)}_{\leq 1} \quad (3.19)$$

$$\leq \frac{1}{2}. \quad (3.20)$$

Since in the above derivation we allow any unitary operation of the form  $U_A \otimes U_B$ , the fully entangled fraction has to fulfil

$$F[(|\psi_A\rangle \otimes |\psi_B\rangle)(\langle\psi_A| \otimes \langle\psi_B|)] \leq \frac{1}{2}. \quad (3.21)$$

□

**Lemma 3.3.3.** *Let  $\mathcal{H}_A$  and  $\mathcal{H}_B$  be two-dimensional Hilbert spaces and let  $\rho$  be a separable mixed state of the combined system, i.e.  $\rho := \rho_A \otimes \rho_B$  for some density operators  $\rho_A$  on  $\mathcal{H}_A$  and  $\rho_B$  on  $\mathcal{H}_B$ . Then, the fully entangled fraction of  $\rho$  is always less than or equal to 0.5.*

*Proof.* By definition, the density matrices  $\rho_A$  and  $\rho_B$  can be written as

$$\rho_A := \sum_i^n p_{A,i} |\psi_{A,i}\rangle \langle\psi_{A,i}| \quad \text{and} \quad (3.22)$$

$$\rho_B := \sum_i^n p_{B,i} |\psi_{B,i}\rangle \langle\psi_{B,i}|, \quad (3.23)$$

where each sum goes over an ensemble of  $n$  pure states  $|\psi_{A,i}\rangle$  and  $|\psi_{B,i}\rangle$  of the systems  $A$  and  $B$  respectively. For these ensembles,  $p_{A,i}$  and  $p_{B,i}$  denote the probabilities with which the systems  $A$  and  $B$  are in state  $|\psi_{A,i}\rangle$  and  $|\psi_{B,i}\rangle$  respectively. With these definitions, we have

$$F(\rho) := F(\rho_A \otimes \rho_B) \quad (3.24)$$

$$= F\left(\left(\sum_i^n p_{A,i} |\psi_{A,i}\rangle \langle\psi_{A,i}| \right) \otimes \left(\sum_i^n p_{B,i} |\psi_{B,i}\rangle \langle\psi_{B,i}| \right)\right) \quad (3.25)$$

$$= F\left(\sum_i^n \sum_j^n p_{A,i} p_{B,j} (|\psi_{A,i}\rangle \otimes |\psi_{B,j}\rangle) (\langle\psi_{A,i}| \otimes \langle\psi_{B,j}|)\right) \quad (3.26)$$

$$\leq \sum_i^n \sum_j^n p_{A,i} p_{B,j} F(|\psi_{A,i}\rangle \otimes |\psi_{B,j}\rangle) (\langle\psi_{A,i}| \otimes \langle\psi_{B,j}|) \quad \text{by Lemma 3.3.1} \quad (3.27)$$

$$\leq \sum_i^n \sum_j^n p_{A,i} p_{B,j} \frac{1}{2} = \frac{1}{2} \sum_i^n p_{A,i} \sum_j^n p_{B,j} = \frac{1}{2} \quad \text{by Lemma 3.3.2.} \quad (3.28)$$

□

## Chapter 4

# Entanglement Distillation Protocols

Given a certain number  $n$  of copies of a particular non-separable state, the goal of Entanglement Distillation is to obtain a number  $m$  of (close to) perfectly entangled states as high as possible using only local operations and, if needed, classical communication. For states that are not perfectly entangled, the best achievable fraction  $m/n$  has to be smaller than 1. This is true by definition: any state that can be converted to a maximally entangled state by LOCC is by itself maximally entangled (See Section 3.1). Furthermore, the optimal fraction  $m/n$  is non-increasing under LOCC since if it could be increased it would not be optimal. Thus, the optimal fraction  $m/n$  serves as an entanglement measure, which is usually called the distillable entanglement  $E_D$ .

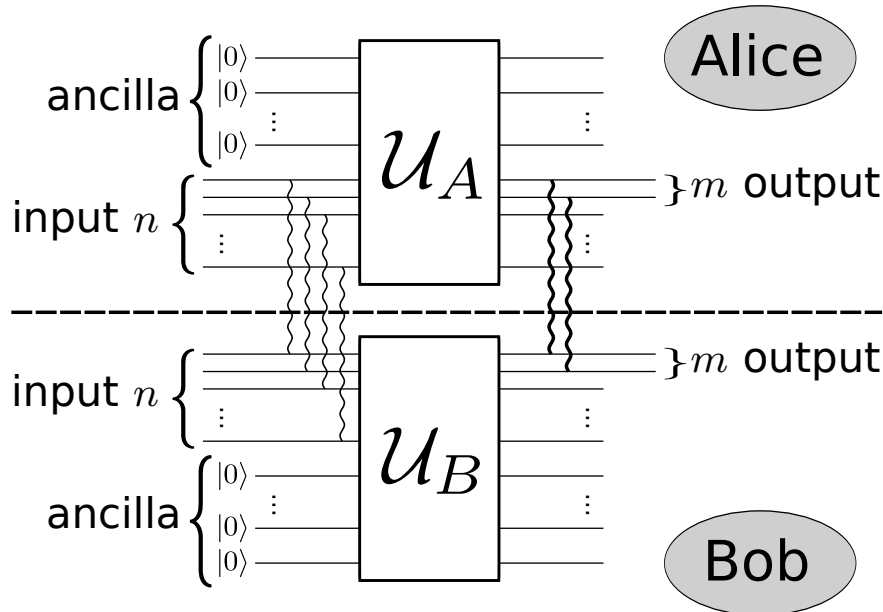
In the context of optimization (see Chapter 5) and in the case when finite  $n$  is considered, it may also be useful to ask the modified question of how much of the initial entanglement can be concentrated in a certain number  $m$  of qubits (where  $m < n$ ) instead of requiring the  $m$  output states to be perfectly entangled. This is the scenario we will consider most in this work.

Table C.1 summarizes the properties of some previously known entanglement distillation protocols.

### 4.1 Single Pair Purification

Protocols exist, that act on a single pair of qubits distributed between Alice and Bob. Examples for such protocols are the Procrustean method, entanglement swapping and local filtering (see Table C.1). These protocols rely on the fact that with a certain measurement procedure one can project the state of the two-qubit system onto a maximally entangled state. This projection belongs to a particular measurement outcome that only occurs with a certain probability. Therefore Alice and Bob have to “post-select” the maximally entangled states, which means that they discard their qubits if the measurement outcomes differ from the one that corresponds to the maximally entangled state. Such a protocol can be executed by local operations and classical communication (LOCC). Since every two states that can be interconverted by LOCC to each other with certainty are considered to be equally entangled, it follows that whenever the probability  $p_{\text{succ}}$  with which a maximally entangled state is obtained by such a single pair purification protocol is smaller than one, the input state has to be less than maximally entangled. This suggests the usefulness of the best achievable  $p_{\text{succ}}$  as an entanglement measure. This (non-additive) entanglement measure is called the entanglement





**Figure 4.1:** General scheme of an entanglement protocol without communication. Entangled Pairs of qubits are connected by a wavy line. The initial entanglement of the  $n$  input qubit pairs shared by Alice and Bob is concentrated into  $m$  pairs of stronger entanglement by the unitary operations  $\mathcal{U}_A$  and  $\mathcal{U}_B$ . The ancilla qubits can be used to perform irreversible operations such as measurements on the  $n$  input qubits as part of these unitary operations.

of single pair purification [23] usually denoted as  $E_s$ .

## 4.2 Protocols without communication

Figure 4.1 shows the general scheme of an entanglement protocol without communication. The entanglement protocol is completely determined by the two unitary operations  $\mathcal{U}_A$  and  $\mathcal{U}_B$ . In order to be able to perform irreversible operations such as measurements on the  $n$  qubits, a number of ancilla qubits can be added.

Among the protocols shown in Table C.1, there are two protocols that work without communication: the Schmidt projection method by Bennet et al [12] for pure states and the No-communication Random Permutation Protocol by Ambainis and Yang [8] for mixed states. The reader may wonder why such protocols can exist at all. In the case of the Schmidt projection method this is possible because Alice and Bob can gain some information about their state by an incomplete measurement on the  $n$  input qubits and use this information to concentrate the entanglement into a number  $m < n$  qubits. In the Random Permutation Protocol, Alice and Bob make use of shared source of random numbers (public coin) and some initially shared perfectly entangled states. The improvement of the fidelity with the Random Permutation Protocol is very limited.

## 4.3 General Limitations and Optimality

The protocols shown in Table C.1 give lower bounds on the distillable entanglement of the states they act on. There also exist several upper bounds on distillable entanglement. First of all since entanglement protocols are a special case of general entanglement

transformations, all limits known to general entanglement transformations apply also for entanglement protocols. As shown in [24], a pure state  $|\psi\rangle$  can be transformed into another pure state  $|\phi\rangle$  if and only if

$$\lambda_\psi \prec \lambda_\phi, \quad (4.1)$$

where  $\lambda_\psi$  and  $\lambda_\phi$  are the vectors of eigenvalues of  $\rho_{\psi,A} = \text{tr}_B|\psi\rangle\langle\psi|$  and  $\rho_{\phi,A} = \text{tr}_B|\phi\rangle\langle\phi|$ . The relation  $\prec$  means that  $\lambda_\psi$  is majorized by  $\lambda_\phi$ , i.e.  $\sum_i(\lambda_\psi^\downarrow)_i \leq \sum_i(\lambda_\phi^\downarrow)_i$ , where  $\lambda_\psi^\downarrow$  ( $\lambda_\phi^\downarrow$ ) have the same elements as  $\lambda_\psi$  ( $\lambda_\phi$ ) but are sorted decreasingly. From the above necessary and sufficient condition for entanglement conversion under LOCC, it is easy to derive that the entropy of entanglement cannot be increased under LOCC. The majorization condition is also discussed in [18, pp. 573–581], where they also pose an exercise to prove a similar condition for entanglement transformation of pure states without the ability to communicate, namely

**Theorem 4.3.1.** (*Exercise 12.22 from [18, p. 579]*) A pure state  $|\psi\rangle$  can be transformed into another pure state  $|\phi\rangle$  without communication if and only if

$$\lambda_\psi \cong \lambda_\phi \otimes \mathbf{x}, \quad (4.2)$$

where  $\mathbf{x}$  is a vector of non-negative elements summing up to 1,  $\lambda_\psi$  and  $\lambda_\phi$  are the vectors of eigenvalues of  $\rho_{\psi,A} = \text{tr}_B|\psi\rangle\langle\psi|$  and  $\rho_{\phi,A} = \text{tr}_B|\phi\rangle\langle\phi|$ . The relation  $\cong$  means that the vectors  $\lambda_\psi$  and  $\lambda_\phi \otimes \mathbf{x}$  have the same elements but possibly with different order.

The proof of Theorem 4.3.1 is postponed to Appendix A. While 4.3.1 is relatively easy to prove for pure states since we can use the Schmidt decomposition to find the relationship between  $\lambda_\psi$  and  $\lambda_\phi$ , it becomes more complicated when one or both of the input and output states of the transformation are mixed states. The Scenario involving mixed states is investigated by the numerical optimization described in Chapter 5.

In [13] it is shown that for an arbitrary *pure* state  $|\psi\rangle$  with entropy of entanglement  $E_{\text{init}}$ , the optimal probability of distilling more than  $nE_{\text{init}}$  maximally entangled states goes to zero as  $n$  goes to infinity. On the other hand, the Schmidt projection method (see Table C.1 and Section 4.4) produces a number of  $m = nE_{\text{init}}$  maximally entangled states as  $n$  approaches infinity. Thus the Schmidt projection method is *asymptotically* optimal. Furthermore, in [13] it is also shown that  $m < nE_{\text{init}}$  is a sufficient condition to distill  $m$  maximally entangled states out of  $n \rightarrow \infty$  copies of *any* pure state.

An overview of this and other previously known limits to the existence of entanglement protocols is given in Table C.2. All of these limits apply to entanglement protocols without communication. Those limits that are also valid for protocols with communication are indicated by an asterisk (\*) in the column denoted as “comm” in Table C.2.

## 4.4 A Note On The Schmidt Projection Method For Two Copies

The Schmidt projection method by Bennet et al [12] is an entanglement distillation method for pure states that works without communication. The procedure is as follows: first, an incomplete measurement is performed to project the system into a subspace where the state is maximally entangled if the measurement outcome  $k$  is larger than 0 and smaller than  $n$ . Then the maximally entangled state is transferred into a standard form such as  $m$  copies of a particular Bell state i.e.  $(|\phi^+\rangle)^{\otimes m}$ .

As pointed out in [12], this procedure only becomes efficient for a large number of copies  $n$ . Nevertheless, there is a non-zero probability of obtaining a maximally

entangled state even for  $n = 2$  copies. In the context of the optimization technique described in Chapter 5, the question arose whether it is possible to concentrate enough entanglement into the subsystem of the first pair of qubits, so that the fully entangled fraction of the mixed state that results from application of the protocol is higher than for one of two copies of a given input state. I.e.:

$$F(\text{tr}_{A_2} \text{tr}_{B_2} [\mathcal{E}(|\Psi_{\text{input}}\rangle \otimes |\Psi_{\text{input}}\rangle)]) \stackrel{?}{>} F(|\Psi_{\text{input}}\rangle), \quad (4.3)$$

where  $\mathcal{E}$  denotes the Schmidt projection method that takes a pure state as input.

For 2 copies, the answer to this question is negative:

**Theorem 4.4.1.** *The Schmidt projection method, if applied on two copies of a pure initial state, does not lead to a state with higher fully entangled fraction than the initial state if no post-selection is allowed.*

Note that this result does not mean the Schmidt projection method is not useful at all for entanglement distillation with two copies of an imperfectly entangled state. There is a non-zero probability of obtaining a measurement result from that one knows that the post-measurement state is a perfectly entangled pure state. It just means that it is necessary to select those outputs of the protocol that have been successful and throw away those that were not successful (post-selection).

Theorem 4.4.1, which is proven in Appendix B, leads to the question whether it is possible at all to increase the fully entangled fraction, if only two copies of a pure state are given as input to any entanglement distillation protocol without communication and without post-selection. This question turns out to be hard to answer analytically, but it is addressed by numerical optimization in Chapter 5.

Interestingly, it is possible to increase the fully entangled fraction of the first pair of qubits if  $n = 3$  copies of  $|\psi\rangle$  are given. It can be done by the following procedure:

**Protocol 4.4.1.** (*Schmidt projection method for 3 copies of a pure state*)

1. Apply the Schmidt projection method on the first two copies.
2. If the method was not successful in obtaining a maximally entangled state, flip the third copy of  $|\psi\rangle$  with the first pair of qubits (conditional swap). If necessary, apply the local unitary transformations on the first qubit in Alice's and Bob's location such that the fidelity of the first pair of qubits w.r.t. a maximally entangled state equals the fully entangled fraction of the initial state.

**Claim 4.4.1.** *Given 3 copies of a pure input state  $|\Psi_{\text{input}}\rangle = c|0+\rangle + s|1-\rangle$ ,  $c, s \in \mathbb{R}$ <sup>1</sup> that has a fully entangled fraction  $F(|\Psi_{\text{input}}\rangle) = \frac{1}{2}(c+s)^2$ , the above described protocol produces a mixed state with a fidelity of  $\frac{1}{2}(1-2c^2s^2)(c+s)^2 + 2c^2s^2 > F(|\Psi_{\text{input}}\rangle)$  if the initial state  $|\Psi_{\text{input}}\rangle$  was entangled, i.e.  $c > 0, s > 0$ .*

*Proof.* Since the Schmidt projection method applied on two copies of  $|\Psi_{\text{input}}\rangle$  produces a maximally entangled state with probability  $2c^2s^2$  (see [12]), and in the other case the protocol swaps the output of the Schmidt projection method with the untouched third copy of the initial state, the resulting mixed state is

$$\rho_{\text{out}} = 2c^2s^2|\phi^+\rangle\langle\phi^+| + (1-2c^2s^2)|\Psi_{\text{input}}\rangle\langle\Psi_{\text{input}}|. \quad (4.4)$$

<sup>1</sup>By the Schmidt decomposition every pure state of two qubits can be brought into this form if the computational basis is chosen appropriately (see e.g. [18, p. 109]).

The fidelity with respect to the Bell state  $|\phi^+\rangle$  of the resulting state is:

$$\langle \phi^+ | \rho_{\text{out}} | \phi^+ \rangle = 2c^2s^2 + (1 - 2c^2s^2)F(|\psi_{\text{input}}\rangle\langle\psi_{\text{input}}|) \quad (4.5)$$

$$= 2c^2s^2 + (1 - 2c^2s^2)(c + s)^2 \quad (4.6)$$

This quantity is larger than  $F(|\psi_{\text{input}}\rangle)$  if  $c, s > 0$  and  $c \neq s$ .  $\square$

Note that Protocol 4.4.1 can also be used to distill entanglement from the following mixed state:

$$\rho_{\text{input}} = \sum_{i=1}^k p_i (|\psi_i\rangle\langle\psi_i|)^{\otimes 3}, \quad (4.7)$$

where  $|\psi_i\rangle = c_i|0+\rangle + s_i|1-\rangle$  with  $c_i^2 + s_i^2 = 1$  and  $0 < c_i < s_i$  for  $i = 1, \dots, k$ . And  $p_i > 0$ ,  $i = 1, \dots, k$  with  $\sum_{i=1}^k p_i = 1$ . This can be easily seen since by Lemma 3.3.1 the fully entangled fraction is less than the weighted sum of the fully entangled fractions of  $|\psi_i\rangle$ ,  $i = 1, \dots, k$  with weights  $p_i$ . Furthermore, the Schmidt projection protocol  $\mathcal{E}$  acts linearly on  $\rho_{\text{input}}$  such that

$$\mathcal{E}(\rho_{\text{input}}) = \sum_{i=1}^k p_i \mathcal{E}(|\psi_i\rangle\langle\psi_i|)^{\otimes 3}. \quad (4.8)$$

Let the output of the protocol be only the first pair of qubits, i.e. tracing out the second and third pair,

$$\rho_{\text{output}} = \text{tr}_{A_{2,3}, B_{2,3}}[\mathcal{E}(\rho_{\text{input}})] \quad (4.9)$$

Thus, the fidelity of the first pair of qubits of the output state  $\rho_{\text{output}}$  will be

$$\langle \phi^+ | \rho_{\text{output}} | \phi^+ \rangle = \sum_{i=1}^k p_i \varphi_i, \quad (4.10)$$

where  $\varphi_i$  is the fidelity one obtains by applying Protocol 4.4.1 on 3 copies of the pure input state  $|\psi_i\rangle$  that is by Claim 4.4.1 larger than the fully entangled fraction of  $|\psi_i\rangle$ . It follows that the fully entangled fraction of  $\rho_{\text{output}}$  must be larger than the fully entangled fraction of  $\rho_{\text{input}}$ .

## Chapter 5

# Numerical Optimization

The task of finding deterministic protocols for entanglement distillation of an arbitrary bipartite state without communication (see Section 4.2) is addressed by the following optimization problem:

**Problem 5.0.1.** (*Optimization Problem*)

Given the input state  $\rho_{input} \in \mathcal{H}_{2n}$ , find  $\mathcal{U}_A \in \mathbb{C}^{n \times n}$  and  $\mathcal{U}_B \in \mathbb{C}^{n \times n}$  which minimize

$$f(\mathcal{U}_A, \mathcal{U}_B) = 1 - \langle \phi^+ | \text{tr}_{S_A} \text{tr}_{S_B} [(\mathcal{U}_A \otimes \mathcal{U}_B) \rho_{input} (\mathcal{U}_A^\dagger \otimes \mathcal{U}_B^\dagger)] | \phi^+ \rangle, \quad (5.1)$$

where  $\text{tr}_{S_A}$  ( $\text{tr}_{S_B}$ ) denotes the partial trace over the subsystem of Alice (Bob) without her (his) first Qubit,

subject to the constraint of  $\mathcal{U}_A, \mathcal{U}_B \in \mathbb{C}^{2^n \times 2^n}$  being unitary matrices, i.e.

$$\mathcal{U}_A^\dagger \mathcal{U}_A = \mathcal{U}_A \mathcal{U}_A^\dagger = \mathcal{U}_B^\dagger \mathcal{U}_B = \mathcal{U}_B \mathcal{U}_B^\dagger = \mathbf{1}. \quad (5.2)$$

The Optimization Problem 5.0.1 can be converted into an unconstrained problem by an appropriate parameterization of the unitary matrices  $\mathcal{U}_A$  and  $\mathcal{U}_B$  (see Section 5.1). A difficulty with this approach is, that parameterizations of unitary matrices are always non-linear and cannot be written as polynomials with a finite number of coefficients. Therefore, this approach requires an efficient algorithm to perform unconstrained non-linear optimization (non-linear programming). Several algorithms exist to perform local non-linear optimization, e.g. Newton's method (see e.g. [25]). In contrast, no algorithm is known, that deterministically performs global optimization of a general non-linear continuous objective function of several variables. In order to circumvent this difficulty, several heuristics can be employed such as starting the Local optimization with a number of randomly distributed initial search points. A class of heuristics that has been quite successful in many applications is the so called evolutionary algorithms. Due to the stochastic nature of evolutionary algorithms, they are well suited for objective functions with a large number of parameters. This work investigates the use of CMA-ES (Covariance Matrix Adaptation - Evolution Strategy) [9], which is a modern evolutionary algorithm for continuous objective functions (Section 5.2). As test cases serve the problems of finding protocols to distill entanglement from 3 or 2 copies of a pure input state in Section 5.3 and 5.4 respectively and from 3 copies of a mixed input state in Section 5.5.

As an alternative approach one could try to directly solve the Optimization Problem 5.0.1. The real valued objective function  $f(\mathcal{U}_A, \mathcal{U}_B)$  is a positive polynomial of

fourth order with complex coefficients and complex-valued variables, which are the elements of the unitary matrices in its argument. The constraints are equalities on positive polynomials of second order (also with complex variables and coefficients). Those polynomials can be converted into polynomials of eighth and fourth order respectively in the real valued elements of the real and imaginary parts of the unitary matrices by substituting the complex numbers by  $z = a + ib$ , for  $a, b \in \mathbb{R}$  and analytically performing the matrix-vector multiplications. Lasserre showed in [26] that polynomial optimization problems can be approximated by a sequence of convex linear matrix inequality (LMI) problems. Furthermore, Waki et. al. [27] proposed how to handle equality constraints and provided a practical implementation of their algorithm [28]. The treatment of Optimization Problem 5.0.1 by means of polynomial optimization is not further investigated in the present work but proposed as subject for future research.

## 5.1 Parameterization of Unitary Matrices

The goal of this section is to find a parameterization

$$\mathcal{P} : \mathbb{R}^k \rightarrow U(N); \mathbf{x} \in \mathbb{R}^k \mapsto \mathbf{U} = \mathcal{P}(\mathbf{x}) \in U(N), \quad (5.3)$$

where  $U(N)$  denotes the group of  $N$ -dimensional unitary matrices i.e.

$$U(N) := \{\mathbf{U} \in \mathbb{C}^{N \times N} \mid \mathbf{U}^\dagger \mathbf{U} = \mathbf{U} \mathbf{U}^\dagger = \mathbf{1}\}. \quad (5.4)$$

It is known from group theory [29], that there exists the exponential map

$$\exp : u(N) \rightarrow U(N); \mathbf{X} \in u(N) \mapsto \mathbf{U} := e^{\mathbf{X}} \in U(N), \quad (5.5)$$

$u(N)$  denotes the corresponding  $N$ -dimensional algebra  $u(N) = \{\mathbf{X} \in \mathbb{C}^{N \times N} \mid \mathbf{X}^\dagger = -\mathbf{X}\}$  and  $e^{\mathbf{X}}$  is the matrix exponential. This exponential map can also be written as

$$\mathbf{U} = e^{i\mathbf{H}}, \quad (5.6)$$

where  $\mathbf{H} = \mathbf{H}^\dagger$  is a hermitean matrix.

Therefore, a simple parameterization of unitary operations is obtained by parameterizing hermitean matrices  $\mathbf{H}$ . This can be done by mapping  $\frac{1}{2}N(N+1)$  real parameters to the elements of a symmetric matrix  $\mathbf{S}$  and  $\frac{1}{2}N(N-1)$  parameters to the elements of a skew-symmetric matrix  $\mathbf{K}$  such that  $\mathbf{H} = \mathbf{S} + i\mathbf{K}$ . In total this parameterization has  $k = N^2$  parameters.

The above described parameterization has a major drawback: the matrix exponential is expensive to compute. Fortunately, there is a divide-and-conquer algorithm found by C. Jarlskog [30, 29] that computes the exponential map (5.5) using  $\mathcal{O}(N^2)$  elementary operations.

Since the computing time an optimization algorithm needs to converge to the optimum strongly depends on the number of parameters  $k$  and the number of dimensions  $N$  grows exponentially with the number of Qubits, it is sometimes useful to restrict the optimization to a subset of all possible solutions. In the case of unitary matrices one can restrict the search to the subset of orthogonal matrices that only have  $N(N-1)$  degrees of freedom in addition to one parameter (the determinant) that can be either plus or minus one. A recursive parameterization of orthogonal matrices of determinant +1 or -1 that is efficient to compute has been found by R. Raffennetti and K. Ruedenberg [31]. The parameterization of orthogonal matrices has the advantage, that the derivatives of the matrix elements with respect to the parameters can be computed and it can be efficiently inverted [32]. The disadvantage is, that the sign of the determinant is an additional binary parameter.

## 5.2 Black-Box Optimization With CMA-ES

In the following, the CMA-ES optimization algorithm [9] is introduced, that has been used to obtain the results presented in Sections 5.3, 5.4 and 5.5. A detailed discussion of CMA-ES is given in [33]. The algorithm was designed to solve a general multivariate single-objective optimization problem with the goal that the user of the algorithm a-priori needs very little knowledge about the objective function. This kind of treatment is called “black-box” optimization (BBO).

The origin of CMA-ES is the so called evolution strategy that was developed in the early 1970’s by Rechenberg and Schwefel in their Ph.D. theses [34, 35]. As for the evolution strategy, CMA-ES maintains a set of strategy parameters that describe how to sample a number  $\lambda$  of guesses of the solution to the optimization problem, i.e. the vector that minimizes the objective function. Following the idea and terminology of biological evolution theory, these guesses are called “children”, “offspring” or simply “population”. For each of these guesses, the objective function is evaluated to get a so called fitness value. Using the ranking based on the objective function value, the  $\mu$  best candidate solutions (“parents”) are selected. To conclude one iteration (also called “generation”), the strategy parameters are updated by machine learning based on the properties of the selected parent solutions as well as information about the previous iterations. This last step of the iteration is called self-adaptation. The entire procedure is repeated many times so that a larger and larger part of the space of possible solution vectors is explored.

In CMA-ES, the  $\lambda$  offspring  $\mathbf{x}_k^{(g)}$  of generation  $g$  are sampled from a multivariate normal distribution: [33]

$$\mathbf{x}_k^{(g)} \sim \mathcal{N}\left(\mathbf{m}^{(g)}, (\sigma^{(g)})^2 \mathbf{C}^{(g)}\right) \quad \text{for } k = 1, \dots, \lambda. \quad (5.7)$$

The strategy parameters are the mean vector  $\mathbf{m}^{(g)}$ , the covariance matrix  $\mathbf{C}^{(g)}$  and a scalar  $\sigma^{(g)}$  that scales the covariance matrix and is thus called “step length”. The mean vector is updated by a weighted average over the  $\mu$  selected parents. The default setting for the number of parents is  $\mu = \frac{1}{2}\lambda$ . It is reasoned in [33] that this is a good choice if the weights are chosen to be linearly decreasing from the parent with the best fitness value to the one among the  $\mu$  selected parents with the worst fitness.

In order to store information about previous iterations that can be used to update the covariance matrix  $\mathbf{C}$  and step length  $\sigma$ , there are two additional strategy parameters, the so called cumulated evolution paths  $\mathbf{p}_c^{(g)}$  and  $\mathbf{p}_\sigma^{(g)}$ . These evolution paths are weighted sums over the difference between the mean vectors  $\mathbf{m}^{(g)}$  and  $\mathbf{m}^{(g+1)}$  of two consecutive iterations (referred to as “steps”). The weights are chosen to be exponentially fading, so that the most recent step gains the highest weight. The evolution paths can be calculated by update rules given in [33]. In the update of  $\mathbf{p}_c^{(g+1)}$ , the effect of the global step size  $\sigma^{(g)}$  on the evolution path is undone, so that this vector only reflects the direction from the mean vector  $\mathbf{m}$  of the previous iteration to the one of the present iteration. The principal components of the covariance matrix are then adapted to  $\mathbf{p}_c^{(g+1)}$ . This update is usually combined with the so called rank- $\mu$  update [36] that takes into account the differences between the strategy mean vector  $\mathbf{m}^{(g)}$  and each of the  $\mu$  best offspring of generation  $g$  separately. Using the rank- $\mu$  update, more information about the every single individual is incorporated into the update of the covariance matrix so that larger population sizes will lead to faster learning of the covariance matrix.

On the other hand,  $\mathbf{p}_\sigma^{(g+1)}$  is calculated by transforming the steps with  $\mathbf{C}^{-1/2}$  in order to negate the effect of the covariance matrix. The magnitude of  $\mathbf{p}_\sigma$  is compared to an analytically calculated expectation value under the assumption that the  $\mu$  best offspring are distributed around the strategy mean vector  $\mathbf{m}^{(g)}$  by the multivariate normal

distribution  $\mathcal{N}(\mathbf{m}^{(g)}, \mathbb{1})$ , where  $\mathbb{1}$  denotes the identity matrix. If the actual evolution path  $\mathbf{p}_\sigma^{(g+1)}$  is longer (shorter) than the expected length, this means that the step length  $\sigma^{(g)}$  was too short (long) and thus will be increased (decreased) for the next iteration.

As explained in [9], the adaptation of the covariance matrix improves the probability for the algorithm to find the global optimum compared to traditional evolution strategies. Namely, the global search property largely depends on the step size, which is adjusted by the self-adaptation part of CMA-ES. A large number of offspring  $\lambda$  should also make the search more global since it increases the density of points that are evaluated in the search space.

### 5.3 Results for 3 copies of a pure initial state with 2 ancilla qubits per party

We want to find entanglement distillation protocols with input given by three copies of the pure state

$$|\psi_{\text{input}}\rangle = \sqrt{0.1}|0+\rangle + \sqrt{0.9}|1-\rangle \quad (5.8)$$

together with two ancilla qubits on Alice's and Bob's location. Thus, the input state that determines Optimization Problem 5.0.1 is

$$\rho_{\text{input}} = (|\psi_{\text{input}}\rangle\langle\psi_{\text{input}}|)^{\otimes 3} \otimes |00\rangle\langle 00| \otimes |++\rangle\langle ++| \quad (5.9)$$

One copy of the input state  $|\psi_{\text{input}}\rangle$  has a fidelity of 0.8. For this problem, we know that we can achieve a fidelity of 0.836 by Protocol 4.4.1, which corresponds to an objective function value of 0.164 provided that Alice and Bob each have two ancilla qubits to do the Schmidt projection measurement. So this problem can serve as a test to evaluate the suitability of the optimization algorithm to find new entanglement distillation protocols.

#### 5.3.1 Optimization over a Single Orthogonal Matrix

In order to reduce the dimensionality of the optimization problem, the number of parameters have been reduced by only optimizing over orthogonal matrices (see Section 5.1) and by setting  $\mathcal{U}_B \stackrel{!}{=} \mathcal{U}_A$  ("symmetric distillation"). Note that Protocol 4.4.1 leads to an orthogonal matrix and is a case of symmetric distillation.

Under these restrictions, the operation of one party on the three local copies and on two ancilla qubits, is represented by an orthogonal matrix of dimension  $d = 2^{3+2} = 32$ . The corresponding parameterization has  $\frac{1}{2}d(d-1) + 1 = 497$  parameters. This number includes one additional parameter, which has been chosen to be the first element of the parameter vector. The sign of this parameter determines the sign of the determinant, whereas the magnitude of the parameter has no effect on the objective function value.

The optimization has been started multiple times, each time with a different initial search point and a different seed of the random number generator.

Interestingly, there were several runs of the optimization that converged to an objective function value of 0.164. This objective function value corresponds to an end state with a fidelity of 0.836 that equals the fully entangled fraction of the output state that is produced by Protocol 4.4.1. Since the fidelity of the output state is higher than the initial fully entangled fraction of 0.8, we conclude that it is possible to find entanglement distillation protocols by the presented optimization method. The optimization runs that resulted in a protocol that achieves a higher fidelity than the initial fully entangled fraction will be called successful optimization runs.



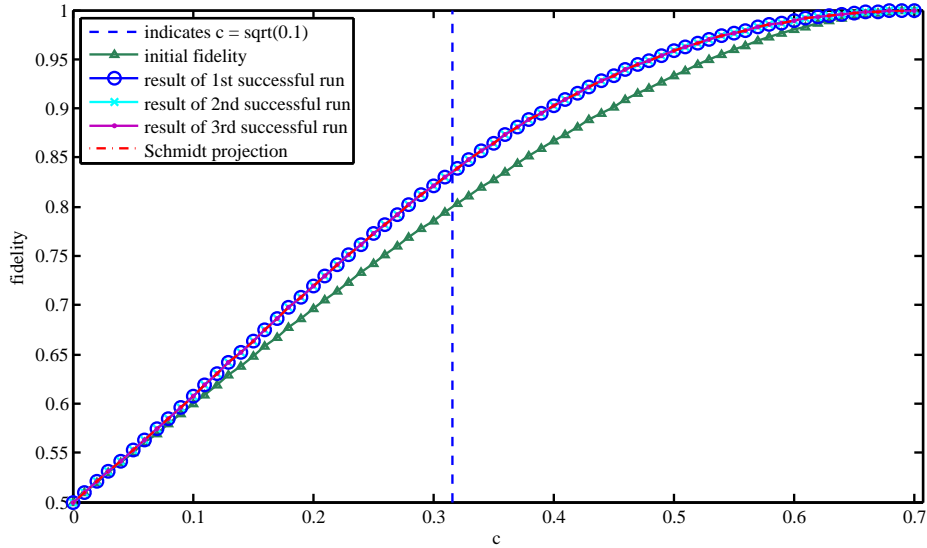


**Figure 5.1:** The fidelity of the state one obtains by applying different protocols on three copies of the input state  $|\psi\rangle = c|0+\rangle + \sqrt{1-c^2}|1-\rangle$  for different values of  $c$ . For comparison, the fidelity of the input state is indicated by the green line with triangles. It can be seen, that all protocols lead to a state of the same fidelity. Three of those protocols have been obtained by numerical optimization using the CMA-ES optimization algorithm. They are referred to as first, second and third successful run. By the term 'Schmidt projection' in the legend, Protocol 4.4.1 is meant. The vertical dashed line indicates  $c = \sqrt{0.1}$  that corresponds to the input state for which these protocols have been optimized in the three successful optimization runs.

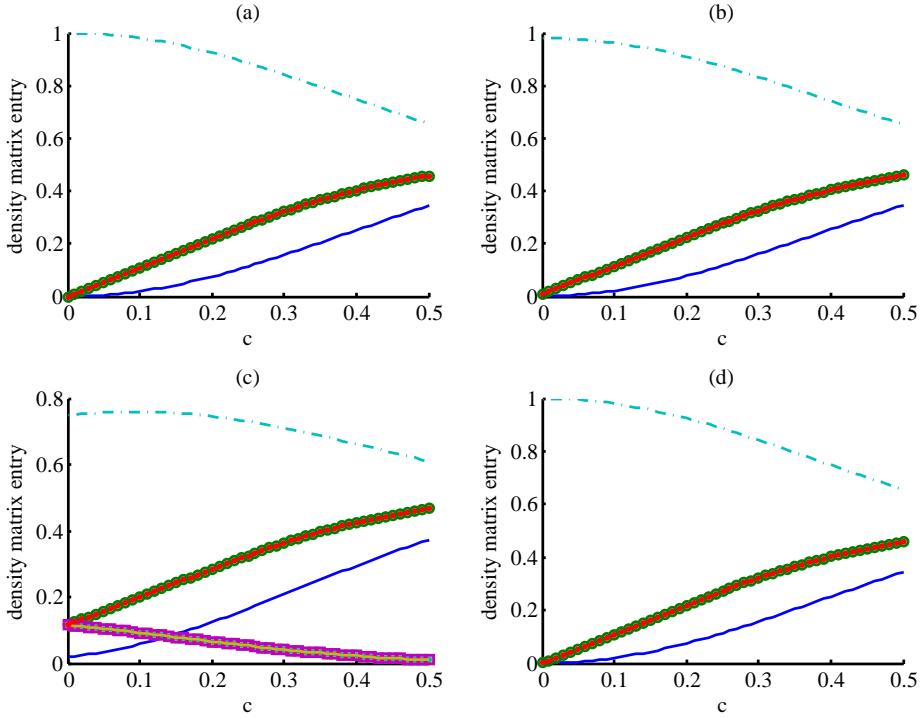
The initial search point of the first and second successful run has been chosen by sampling from a Gaussian distribution around the zero vector with a standard deviation of 0.0814. By the parameterization of orthogonal matrices, the zero-vector corresponds to the identity matrix. For the third successful run, the initial search point has been chosen to be exactly the zero vector. Each of these runs have been started with an initial step width of  $\sigma = 0.01$  that turned out to lead to faster convergence compared with larger step widths. The optimal initial step width is hard to find due to the high computational cost of each optimization run.

Figure 5.1 shows the fidelity that one gets if the protocols found by the three optimization runs are applied on initial states of the form  $c|0+\rangle + \sqrt{1-c^2}|1-\rangle$ . for different values of  $c$ . Keep in mind that the optimization has been performed for an initial state with  $c = 0.1$  (5.8). While the unitary matrices that make up these protocols differ, the final states obtained by these protocols have the same fidelity for every possible input state that equals to the fidelity achieved by Protocol 4.4.1. It can be seen from Figure 5.2, that the density matrices of the end states of the protocols found by the first and third successful run are essentially (up to small deviations) the same as for the end state of Protocol 4.4.1.

While these runs converged to the same objective function value, the determined orthogonal matrices differ between each run. This is illustrated by Figure 5.3.

Furthermore, all of these optimization runs show a slightly different convergence behaviour. It can be seen from Figure 5.4, that the convergence of all optimization runs has stalled near to the initial fitness of 0.2 before the optimization converged to the final fitness value of 0.164 and reached the stopping criteria. The first and the second run needed about 10000 function evaluations until the optimization came close to the final objective function value, whereas in the third run, the fitness value has stalled over a longer period of about  $0.9 \times 10^5$  function evaluations.

Only those optimization runs were successful, that have been started with an initial



**Figure 5.2:** Plots of the elements of the density matrices of the output state obtained by applying four different protocols on three copies of the input state  $|\psi\rangle = c|0+\rangle + \sqrt{1-c^2}|1-\rangle$  for different values of  $c$ . Only those elements of the  $4 \times 4$  real density matrix that considerably differ from zero are shown. Panel (a): Protocol 4.4.1, Panel (b), (c) and (d): first second and third successful run of the CMA-ES optimization algorithm. Solid blue line:  $\rho_{1,1}$ , green circles with red dots:  $\rho_{4,1}$  and  $\rho_{1,4}$ , dash-dotted cyan line:  $\rho_{4,4}$ , magenta squares with brown line in Panel (c):  $\rho_{2,2}$ ,  $\rho_{3,2}$ ,  $\rho_{2,3}$  and  $\rho_{3,3}$ . This figure reveals, that only the protocol of the second successful optimization run leads to a different density matrix than the others.

parameter vector that is close to the zero vector. For those optimization runs for which the elements of the parameter vector have been chosen to be uniformly distributed in the range  $[-\pi, +\pi]$ , the optimization converged to an objective function value of 0.203. This value corresponds to a fidelity of 0.797, which is above the initial fidelity of 0.8. In some cases the optimization simply converged to a fitness value 0.2 that corresponds exactly to the input fidelity and also could be a local minimum. Table C.3 gives an overview over all optimization runs that have been performed.

A possible explanation for it to be beneficial to choose the initial parameters close to zero may be that due to the angular nature of the parameterization of orthogonal matrices, parameters close to zero or a multiple of  $\pi$  will lead to sparse matrices. As can be seen from Figure 5.3, the optimal orthogonal matrices are semi-sparse in the sense that in each column there is a particular element that has a much larger magnitude (from 2 to  $10^5$  times larger) than the other non-zero elements of the column.

### 5.3.2 Unrestricted Optimization over 2 Unitary Matrices

In this section, we present the results of the optimization over two different unitary matrices  $\mathcal{U}_A$  and  $\mathcal{U}_B$ , i.e. without restriction to orthogonal matrices. To do the optimization, the parameterization of unitary matrices presented in Section 5.1 was used. Since each unitary matrix has  $N^2$  degrees of freedom, where  $N = 2^n$  is the dimension of the Hilbert space of  $n = 5$  qubits, we have 2048 parameters in total.

Table C.4 gives an overview of all optimization runs that have been performed for

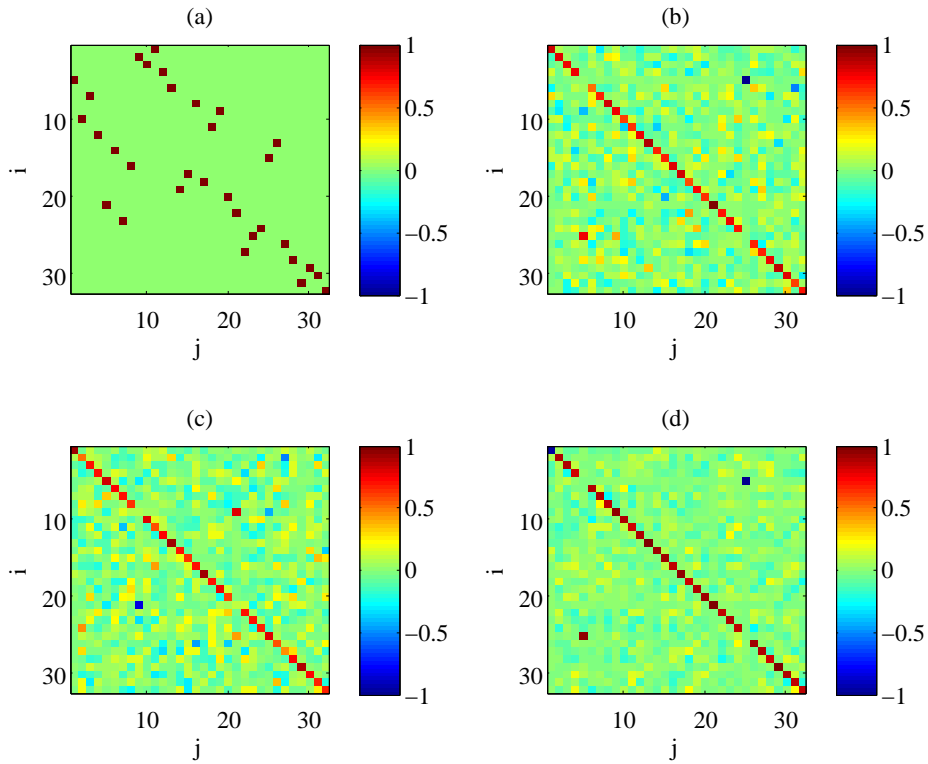


**Figure 5.3:** Visualization of four different orthogonal  $32 \times 32$  matrices that all lead to a state with the same increased fully entangled fraction if simultaneously applied by Alice and Bob on their part of 3 copies of an initially entangled pure state together with two local ancilla qubits per party. The color of each pixel indicates the value of the corresponding matrix entry  $(\mathbf{U})_{i,j}$ . (a) is determined by hand according to Protocol 4.4.1. (b), (c) and (d) are the results of the first, second and third successful run of the optimization with CMA-ES for different initial search points and seeds of the random number generator.

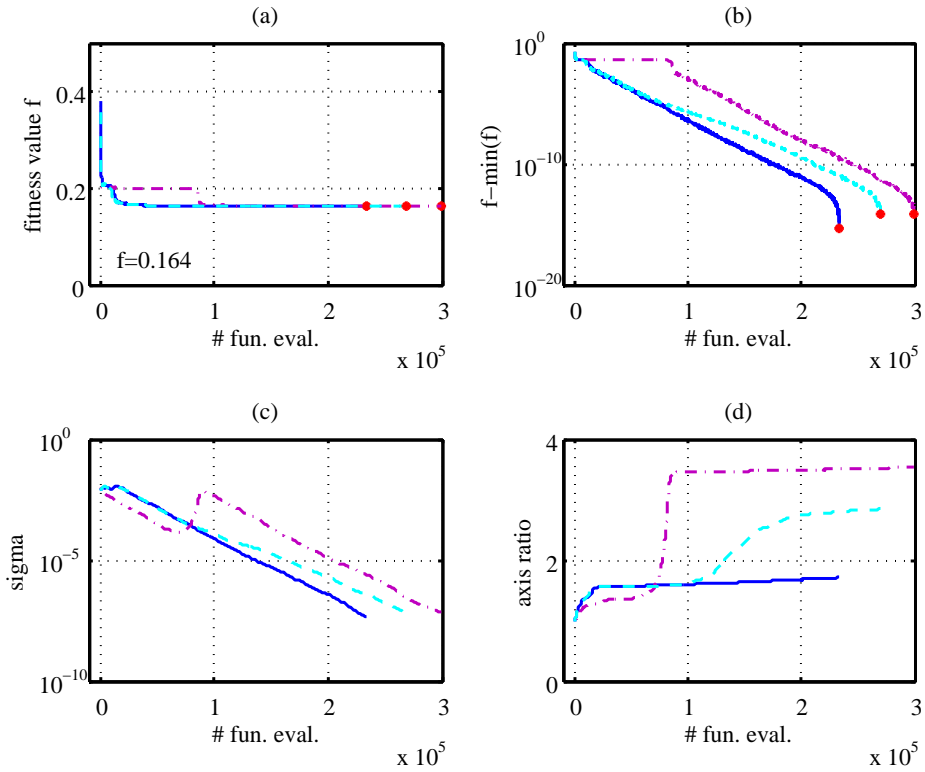


**Figure 5.4:** Convergence behaviour of three runs of the CMA-ES algorithm when used to find an entanglement distillation protocol without communication for 3 copies of a pure state. The optimization was limited to orthogonal matrices and the operations performed by Alice and Bob have been constrained to be the same. The dimensionality of the search space is 497. The fully entangled fraction of the given input state is 0.8, which corresponds to a fitness value of  $f = 0.2$ . The best fidelity achieved was 0.836, which corresponds to a fitness value of  $f = 0.164$ . The blue solid line corresponds to the first successful run, the cyan dashed line to the second and the magenta dashed-dotted line to the third run. The abscissae correspond to the number of objective function evaluations that have been done by the black-box optimization algorithm to reach the corresponding state. Panel (a): the best objective function value found after each iteration. Panel (b): the difference to the final objective function value. Panel (c): the parameter  $\sigma$  of the CMA-ES algorithm, by which the standard deviations of the sampling distribution are scaled (step size). Panel (d): the ratio between the longest and shortest principle axis length of the covariance matrix of the sampling distribution.

the unrestricted optimization. As for the symmetric orthogonal case (Section 5.3.1), it depends on the starting point whether the optimization converges to a protocol that is successful in producing a state below the initial fidelity. But unlike the orthogonal case, the initial parameters do not have to be close to zero. It can be seen from Figure 5.5, that the behaviour of the self-adaptation of  $\sigma$  and the covariance matrix is very similar for two runs with different starting point, even if one run is successful and the other fails. The best protocol that has been found within the limited number of function evaluations for the general unitary case, produces a state with fidelity 0.83272 from the input state (run 8.2 in Table C.4). This value is close to 0.836, which is the fidelity achieved by Protocol 4.4.1. Figure 5.6 shows that the unitary matrices of the protocol found by the optimization are sparse and from Figure 5.7 it can be seen that the found protocol does not perform as good as Protocol 4.4.1 especially for input states that are close to maximally entangled (i.e.  $c \approx \frac{1}{\sqrt{2}}$  in Equation (5.8)) this contrasts with the case where the optimization was restricted to symmetric distillation by orthogonal matrices (c.f. Figure 5.1). Because the number of function evaluations needed to reach the best found objective function value (“needed # f.e.” in Table C.4) is close to the total number of function evaluations that have been performed, we expect that the solution can be improved by running the optimization algorithm for a longer time.

## 5.4 Results for 2 copies of a pure initial state

For the case of only two copies of a pure input state we have shown in Section 4.4, that the Schmidt projection cannot be used to increase the fully entangled fraction without post-selection. Thus, it is an interesting question whether it is possible to find another entanglement distillation protocol that can perform this task. However, none of the tried optimization runs performed on two copies of the state  $0.1|0+\rangle + 0.9|1-\rangle$  resulted in a protocol that leads to a state with higher fidelity than the fully entangled 0.2 of the initial state (see Table C.5). This is a sign that possibly there is no non-interactive protocol that increases the fully entangled fraction of two copies of a pure input state.

## 5.5 Results for 3 copies of a Werner state

It has been tried to use the same optimization method as used for 3 copies of a pure state (Section 5.3) to distill entanglement from 3 copies of a mixed state. The state chosen for this purpose was the Werner state:

$$\rho_{\text{input}} = \left(1 - \frac{3}{4}p\right) |\phi^+\rangle\langle\phi^+| + \frac{1}{4}p (|\phi^-\rangle\langle\phi^-| + |\psi^+\rangle\langle\psi^+| + |\psi^-\rangle\langle\psi^-|). \quad (5.10)$$

For the optimization  $p$  in (5.10) has been fixed to a value of  $p = 0.1$ . This state has an initial fidelity w.r.t.  $|\phi^+\rangle$  of 0.925, which corresponds to a fitness value of 0.075. We know from [8] that the maximal fidelity we can hope to produce from any number of copies of the Werner state  $\rho_{\text{input}}$  (5.10) is upper bounded by  $1 - \frac{p}{2} = 1 - 0.05 = 0.95$  (see Table C.2). It can be seen from Table C.6, that none of the performed optimization runs was successful. The problem is, that the computational complexity of the objective function evaluation is higher than for the case of a pure input state: In the former case one only has to perform matrix vector multiplication, which has complexity  $\mathcal{O}(N^2)$  where  $N$  is the dimension of the Hilbert space. On the other hand, in order to apply the unitary operations on the mixed input state  $\rho_{\text{input}}$  one has to calculate  $\mathbf{U}\rho_{\text{input}}\mathbf{U}^\dagger$ , which involves two matrix multiplications. For that, the number of elementary operations is

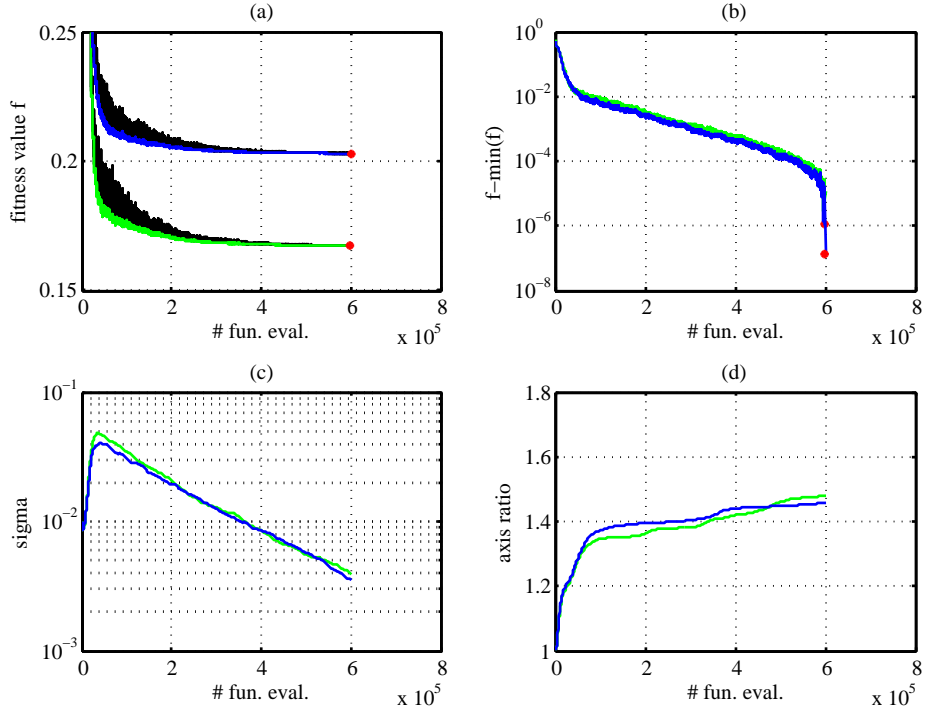


**Figure 5.5:** Convergence behaviour of three runs of the CMA-ES algorithm when used to find an entanglement distillation protocol without communication for 3 copies of a pure state. The search space is 2048-dimensional, which corresponds to the general case of optimization over 2 unitary matrices. The fully entangled fraction of the given input state is 0.8, which corresponds to a fitness value of  $f = 0.2$ . Each of the runs shown in this figure has a different starting point chosen uniformly between  $-\pi$  and  $+\pi$ . The green line corresponds to the first successful run (id 8.2 in Table C.4), the blue line to an unsuccessful run (id 15.1 in Table C.4). The abscissae correspond to the number of objective function evaluations that have been performed by the black-box optimization algorithm to reach the corresponding state. Panel (a): coloured lines show the best objective function value found after each iteration (black lines show the fitness of the worst offspring in the corresponding iteration). Panel (b): the difference to the final objective function value. Panel (c): the parameter  $\sigma$  of the CMA-ES algorithm, by which the standard deviations of the sampling distribution are scaled (step size). Panel (d): the ratio between the longest and shortest principle axis length of the covariance matrix of the sampling distribution.

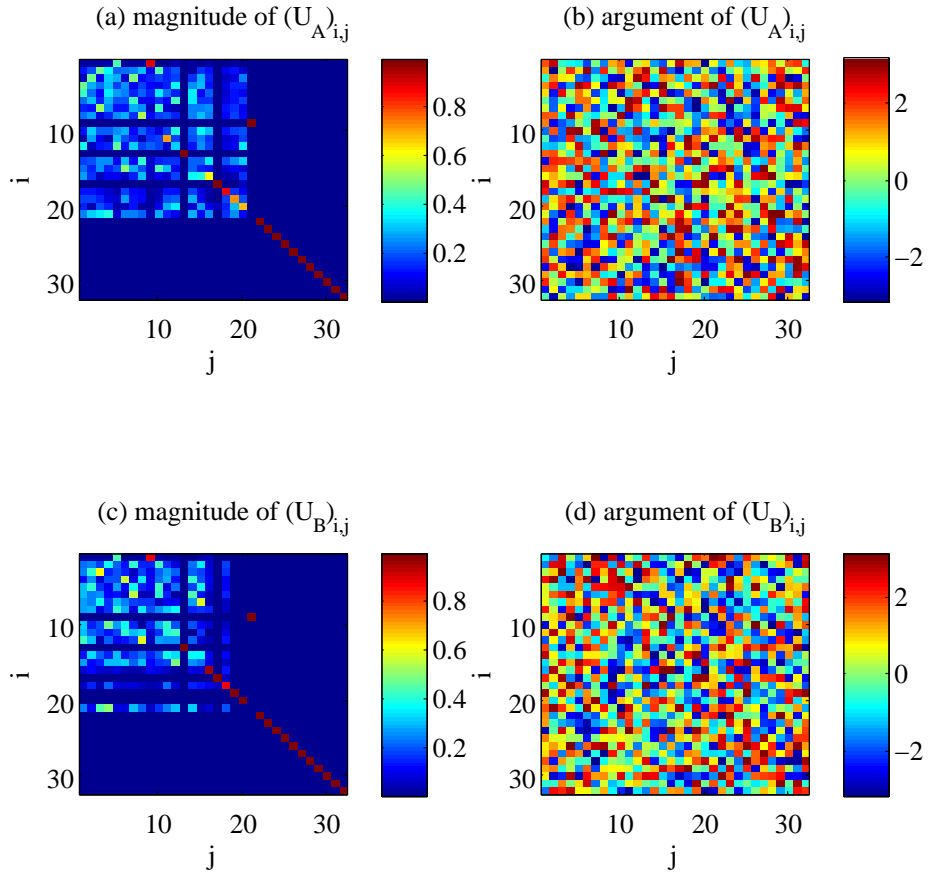


**Figure 5.6:** Visualization of the  $32 \times 32$  unitary matrices  $U_A$  and  $U_B$  found by optimization run 8.2 shown in Table C.4. If  $U_A$  ( $U_B$ ) is applied by Alice (Bob) on her (his) part of 3 copies of the pure state (5.8) together with two local ancilla qubits per party, a fidelity of 0.83272 results. Panel (a): the magnitude of the complex entries of  $U_A$ . Panel (b): the argument  $\arg((U_A)_{i,j}) = \arctan(\text{Im}((U_A)_{i,j})/\text{Re}((U_A)_{i,j}))$ . Panel (c): the magnitude of the complex entries of  $U_B$ . Panel (d): the argument  $\arg((U_B)_{i,j}) = \arctan(\text{Im}((U_B)_{i,j})/\text{Re}((U_B)_{i,j}))$ .

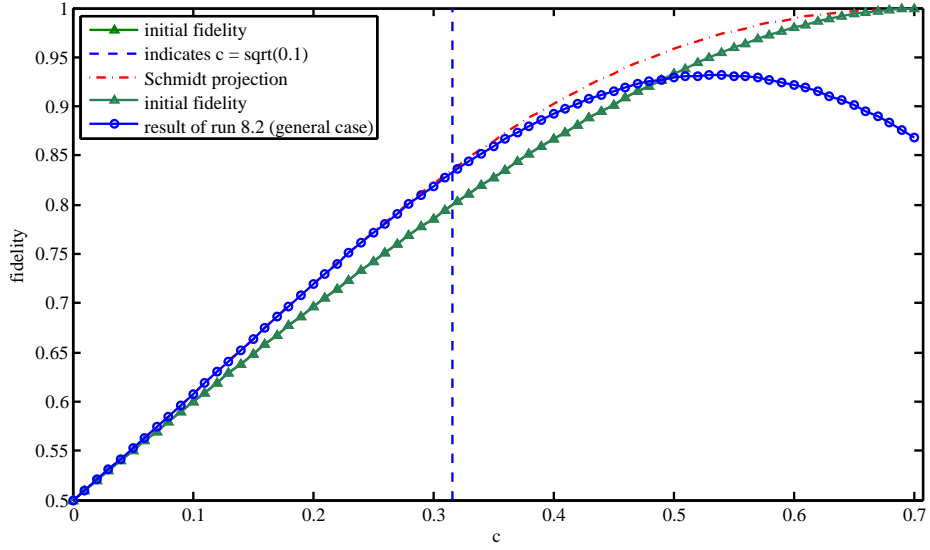


**Figure 5.7:** The fidelity of the state one obtains by applying different protocols on three copies of the input state  $|\psi\rangle = c|0+\rangle + \sqrt{1-c^2}|1-\rangle$  for different values of  $c$  compared to the initial fidelity indicated by the green line with triangles. The performance of the best protocol obtained by numerical optimization over general unitary matrices with limited number of function evaluations (optimization run 8.2 in Table C.4) is indicated by the blue solid line with circles. By the term 'Schmidt projection' in the legend, Protocol 4.4.1 is meant. The vertical dashed line indicates  $c = \sqrt{0.1}$  corresponding to the input state for which optimization run 8.2 has been performed.

on the order of  $\mathcal{O}(N^3)$  with the naive approach <sup>1</sup>.

<sup>1</sup>There exist algorithms for matrix-matrix multiplication with lower complexity such as Strassen's algorithm [37] for which the number of scalar multiplications is on the order of  $\mathcal{O}(N^{\log_2 7})$ .



## Chapter 6

# Conclusions

After summarizing the properties of previously known entanglement distillation protocols and limits to the distillability with and without communication, we have investigated the use of the Schmidt projection method without communication for the cases where only 2 or 3 copies of an entangled state are given. It is possible to increase the fully entangled fraction with the Schmidt projection without post-selection if and only if more than two copies of an entangled pure state are given. We derived a non-interactive entanglement distillation protocol for mixed states from the Schmidt projection method for three copies of a pure input state. Furthermore, we demonstrated the possibility to find an equivalent protocol to the Schmidt projection method for 3 copies by numerical optimization. For 2 copies of a pure input state the numerical optimization was unsuccessful, indicating that no protocol for 2 copies of an entangled pure state that increases the fully entangled fraction exists. Finally, we investigated the performance of the optimization algorithm if the input state is a mixed state.

# Acknowledgements

Many thanks go to my advisor Dejan Dukaric for the great assistance he gave me during the time I was working on the present project, for the patience he had in answering my numerous questions and giving the present work the right direction. My special gratitude belongs to Prof. Stefan Wolf for the opportunity to do the present thesis in his group and for the well understandable and motivating lectures he held at ETH Zürich. His lectures have sparked my interest in quantum information and computation as well as general information science.

# Appendix A

## Proof of Theorem 4.3.1

We are going to proof Theorem 4.3.1:

$$|\psi\rangle \text{ can be non-interactively transformed to } |\phi\rangle \iff \lambda_\psi \cong \lambda_\phi \otimes \mathbf{x}, \quad (\text{A.1})$$

where the elements of vector  $\mathbf{x}$  are non-negative and sum up to 1.

*Proof.* “ $\Leftarrow$ ”: Assume that the right hand side of Equivalence (A.1) is true for some pure states  $|\psi\rangle$  and  $|\phi\rangle$ . Let  $|\psi_E\rangle$  be some pure state with  $\rho_{\psi_E,B} = \text{tr}_B|\psi_E\rangle\langle\psi_E|$  having eigenvalues given by the vector  $\mathbf{x}$  and let  $|\psi_R\rangle := |\phi\rangle \otimes |\psi_E\rangle$ . Furthermore, let the density operator  $\rho_{\psi_R,A} = \text{tr}_B|\psi_R\rangle\langle\psi_R|$  of Alice’s subsystem have eigenvalues given by the vector  $\lambda_\psi \otimes \mathbf{x}$ .

The Schmidt decomposition (see e.g. [18, p. 109]) of any bipartite state  $|\phi\rangle$  is

$$|\phi\rangle = \sum_{i=1}^d \sqrt{c_i} |\varphi_{A,i}\rangle |\varphi_{B,i}\rangle, \quad (\text{A.2})$$

for orthogonal sets of basis vectors  $\{|\varphi_{A,i}\rangle | i = 1, \dots, d\}$  and  $\{|\varphi_{B,i}\rangle | i = 1, \dots, d\}$ , where  $d$  is the dimension of the Hilbert space describing Alice’s and Bob’s subsystem (which for simplicity and without loss of generality are assumed to be of the same dimensionality) and  $\mathbf{c} \in \mathbb{R}^d$  is the vector of squared Schmidt coefficients with  $\sum_i^d c_i = 1$ . The corresponding density matrix is

$$|\phi\rangle\langle\phi| = \sum_{i=1}^d \sum_{j=1}^d \sqrt{c_i c_j} |\varphi_{A,i}\rangle\langle\varphi_{A,j}| \otimes |\varphi_{B,i}\rangle\langle\varphi_{B,j}|. \quad (\text{A.3})$$

Thus, the partial trace over Bob’s subsystem is

$$\rho_{\phi,A} = \text{tr}_B |\phi\rangle\langle\phi| = \sum_{i=1}^d c_i |\varphi_{A,i}\rangle\langle\varphi_{A,i}|. \quad (\text{A.4})$$

So the squared Schmidt coefficients are exactly the eigenvalues of  $\rho_{\phi,A}$ . By the assumption that for the state  $|\psi_R\rangle$  the density matrix of Alice’s subsystem has the same eigenvalues as for the state  $|\psi\rangle$ , it follows that the Schmidt coefficients of  $|\psi_R\rangle$  and  $|\psi\rangle$  are the same. So to convert  $|\psi\rangle$  into  $|\psi_R\rangle$  Alice and Bob just have to apply local unitary operations  $\mathbf{U}_A$  and  $\mathbf{U}_B$  that transform the orthogonal sets of basis vectors  $\{|\varphi_{A,i}\rangle | i = 1, \dots, d\}$  and  $\{|\varphi_{B,i}\rangle | i = 1, \dots, d\}$  from the Schmidt decomposition of  $|\psi\rangle$  into the ones of the Schmidt decomposition of  $|\psi_R\rangle$ . Finally,  $|\phi\rangle$  can be obtained by the partial trace over the subsystem of  $|\psi_E\rangle$  in  $|\psi_R\rangle = |\phi\rangle \otimes |\psi_E\rangle$ .

“ $\implies$ ”: Let us assume that the pure state  $|\psi\rangle$  has been converted into the pure state  $|\phi\rangle$  without communication. It follows that

$$|\psi_R\rangle = |\phi\rangle \otimes |\psi_E\rangle = (\mathbf{U}_A \otimes \mathbf{U}_B)|\psi\rangle. \quad (\text{A.5})$$

From the derivation above, we know that the vectors  $\lambda_\psi$  and  $\lambda_{\psi_R}$  are equal to the vector of squared Schmidt coefficients of  $|\psi\rangle$  and  $|\psi_R\rangle$  respectively. It is easy to see that the local unitary transformation  $\mathbf{U}_A \otimes \mathbf{U}_B$  does not change the values of the Schmidt coefficients of  $|\psi\rangle$ . As above, we define  $\mathbf{x}$  to be the vector of eigenvalues of  $\rho_{\psi_E, A} = \text{tr}_B |\psi_E\rangle\langle\psi_E|$ . Since

$$\text{tr}_B |\psi_R\rangle\langle\psi_R| = \text{tr}_B [|\phi\rangle\langle\phi| \otimes |\psi_E\rangle\langle\psi_E|] = \rho_{\phi, A} \otimes \rho_{\psi_E, A}, \quad (\text{A.6})$$

it follows that  $\lambda_\psi \cong \lambda_\phi \otimes \mathbf{x}$

□

## Appendix B

### Proof of Theorem 4.4.1

In the following, the mathematical statement and proof of Theorem 4.4.1 is given.

**Definition B.0.1.** Let the Schmidt-Projection measurement be defined by the measurement operators  $P_0 := P_{0,A} \otimes P_{0,B}$ ,  $P_1 := P_{1,A} \otimes P_{1,B}$ ,  $P_2 := P_{2,A} \otimes P_{2,B}$  where

$$P_{0,A} := |00\rangle\langle 00|, \quad P_{0,B} := |++\rangle\langle ++|, \quad (\text{B.1})$$

$$P_{1,A} := |01\rangle\langle 01| + |10\rangle\langle 10|, \quad P_{1,B} := |+-\rangle\langle +-| + |-+\rangle\langle -+|, \quad (\text{B.2})$$

$$P_{2,A} := |11\rangle\langle 11|, \quad P_{2,B} := |--\rangle\langle --|. \quad (\text{B.3})$$

The subscripts of the projection operators denote the measurement outcomes.

**Theorem B.0.1.** Mathematical statement of Theorem 4.4.1:

Let  $|\Psi_{\text{input}}\rangle := c|0+\rangle + s|1-\rangle \in \mathcal{H}_A \otimes \mathcal{H}_B$  with  $c, s \in \mathbb{R}$ ,  $c^2 + s^2 = 1$ , where  $|0\rangle$  and  $|1\rangle$  are orthogonal states in the two-dimensional Hilbert space  $\mathcal{H}_A$  while  $|+\rangle$  and  $|-\rangle$  are orthogonal states in the two-dimensional Hilbert space  $\mathcal{H}_B$ . Based on that, let  $|\Psi_{\text{copy}}\rangle := (|\Psi_{\text{input}}\rangle)^{\otimes 2} \in \mathcal{H}_{A_1} \otimes \mathcal{H}_{B_1} \otimes \mathcal{H}_{A_2} \otimes \mathcal{H}_{B_2}$ , where  $\mathcal{H}_{A_1} \otimes \mathcal{H}_{B_1}$  and  $\mathcal{H}_{A_2} \otimes \mathcal{H}_{B_2}$  denote the Hilbert spaces of the first and second copy respectively. Furthermore let  $\rho_{\text{pm}}$  be the state of the system after a Schmidt-Projection measurement (Definition B.0.1). Then

$$F(|\Psi_{\text{input}}\rangle\langle \Psi_{\text{input}}|) > \max_{\mathcal{U}_A, \mathcal{U}_B} F(\text{tr}_{A_2}[\text{tr}_{B_2}[(\mathcal{U}_A \otimes \mathcal{U}_B)\rho_{\text{pm}}(\mathcal{U}_A^\dagger \otimes \mathcal{U}_B^\dagger)]]), \quad (\text{B.4})$$

where  $F(\cdot)$  denotes the fully entangled fraction (Definition 3.3.1),  $\mathcal{U}_A$  denotes an arbitrary unitary operator on the subspace  $\mathcal{H}_{A_1} \otimes \mathcal{H}_{A_2}$  whereas  $\mathcal{U}_B$  denotes an arbitrary unitary operator on  $\mathcal{H}_{B_1} \otimes \mathcal{H}_{B_2}$  and  $\text{tr}_{A_2}[\cdot]$  and  $\text{tr}_{B_2}[\cdot]$  denote the partial trace over the subspaces  $\mathcal{H}_{A_2}$  and  $\mathcal{H}_{B_2}$ .

Note that the ‘‘standardization process’’ as described in [12] is not probabilistic in this special case of only two given copies of the initial state, since if the measurement outcome of the Schmidt-Projection measurement (Definition B.0.1) is 1, then the corresponding state can be transformed into a maximally entangled state with local unitary operations that are applied before tracing out one of the entangled pairs of qubits.

*Proof.* Since

$$|\Psi_{\text{copy}}\rangle := (|\Psi_{\text{input}}\rangle)^{\otimes 2} = c^2|00++\rangle + s^2|11--\rangle + cs(|01+-\rangle + |10-+\rangle) \quad (\text{B.5})$$

$$= c^2|00++\rangle + s^2|11--\rangle + \sqrt{2}cs|\psi_1\rangle \quad (\text{B.6})$$

with  $|\psi_1\rangle := \frac{1}{\sqrt{2}}(|01+-\rangle + |10-+\rangle)$  the state  $\rho_{\text{pm}}$  after application of the Schmidt-Projection measurement (Definition B.0.1) is

$$\rho_{\text{pm}} = c^4|00++\rangle\langle 00++| + s^4|11--\rangle\langle 11--| + 2c^2s^2|\psi_1\rangle\langle\psi_1| \quad (\text{B.7})$$

$$= c^4|00\rangle\langle 00| \otimes |++\rangle\langle ++| \quad (\text{B.8})$$

$$+ s^4|11\rangle\langle 11| \otimes |--\rangle\langle --| \quad (\text{B.9})$$

$$+ 2c^2s^2|\psi_1\rangle\langle\psi_1|. \quad (\text{B.10})$$

Therefore, the state after application of the unitary operator  $\mathcal{U}_A \otimes \mathcal{U}_B$  is

$$\tilde{\rho}_{\text{pm}} := (\mathcal{U}_A \otimes \mathcal{U}_B)\rho_{\text{pm}}(\mathcal{U}_A^\dagger \otimes \mathcal{U}_B^\dagger) \quad (\text{B.11})$$

$$= c^4\mathcal{U}_A|00\rangle\langle 00|\mathcal{U}_A^\dagger \otimes \mathcal{U}_B|++\rangle\langle ++|\mathcal{U}_B^\dagger \quad (\text{B.12})$$

$$+ s^4\mathcal{U}_A|11\rangle\langle 11|\mathcal{U}_A^\dagger \otimes \mathcal{U}_B|--\rangle\langle --|\mathcal{U}_B^\dagger \quad (\text{B.13})$$

$$+ 2c^2s^2(\mathcal{U}_A \otimes \mathcal{U}_B)|\psi_1\rangle\langle\psi_1|(\mathcal{U}_A^\dagger \otimes \mathcal{U}_B^\dagger). \quad (\text{B.14})$$

$$= c^4|\varphi_0^A\rangle\langle\varphi_0^A| \otimes |\varphi_0^B\rangle\langle\varphi_0^B| \quad (\text{B.15})$$

$$+ s^4|\varphi_2^A\rangle\langle\varphi_2^A| \otimes |\varphi_2^B\rangle\langle\varphi_2^B| \quad (\text{B.16})$$

$$+ 2c^2s^2|\tilde{\psi}_1\rangle\langle\tilde{\psi}_1|. \quad (\text{B.17})$$

with  $|\varphi_0^A\rangle := \mathcal{U}_A|00\rangle$ ,  $|\varphi_0^B\rangle := \mathcal{U}_B|++\rangle$ ,  $|\varphi_2^A\rangle := \mathcal{U}_A|11\rangle$ ,  $|\varphi_2^B\rangle := \mathcal{U}_B|--\rangle$  and  $|\tilde{\psi}_1\rangle := (\mathcal{U}_A \otimes \mathcal{U}_B)|\psi_1\rangle$ .

Now the partial trace (linear operator) over the second copy of the distributed pair of qubits is

$$\rho_{\text{output}} := \text{tr}_{A_2}[\text{tr}_{B_2}[\tilde{\rho}_{\text{pm}}]] \quad (\text{B.18})$$

$$= c^4(\text{tr}_{A_2}[|\varphi_0^A\rangle\langle\varphi_0^A|]) \otimes (\text{tr}_{B_2}[|\varphi_0^B\rangle\langle\varphi_0^B|]) \quad (\text{B.19})$$

$$+ s^4(\text{tr}_{A_2}[|\varphi_2^A\rangle\langle\varphi_2^A|]) \otimes (\text{tr}_{B_2}[|\varphi_2^B\rangle\langle\varphi_2^B|]) \quad (\text{B.20})$$

$$+ 2c^2s^2\text{tr}_{A_2}[\text{tr}_{B_2}[|\tilde{\psi}_1\rangle\langle\tilde{\psi}_1|]] \quad (\text{B.21})$$

$$= c^4\rho_{0,A} \otimes \rho_{0,B} + s^4\rho_{2,A} \otimes \rho_{2,B} + 2c^2s^2\rho_1, \quad (\text{B.22})$$

with  $\rho_{0,A} := \text{tr}_{A_2}[|\varphi_0^A\rangle\langle\varphi_0^A|]$ ,  $\rho_{0,B} := \text{tr}_{B_2}[|\varphi_0^B\rangle\langle\varphi_0^B|]$ ,  $\rho_{2,A} := \text{tr}_{A_2}[|\varphi_2^A\rangle\langle\varphi_2^A|]$ ,  $\rho_{2,B} := \text{tr}_{B_2}[|\varphi_2^B\rangle\langle\varphi_2^B|]$  and  $\rho_1 := \text{tr}_{A_2}[\text{tr}_{B_2}[|\tilde{\psi}_1\rangle\langle\tilde{\psi}_1|]]$ .

Because of Lemma 3.3.1, Lemma 3.3.3 and because  $F(\cdot) \leq 1$  by definition, the following inequalities hold

$$F(\rho_{\text{output}}) \leq c^4F(\rho_{0,A} \otimes \rho_{0,B}) \quad (\text{B.23})$$

$$+ s^4F(\rho_{2,A} \otimes \rho_{2,B}) \quad (\text{B.24})$$

$$+ 2c^2s^2F(\rho_1) \quad \text{by Lemma 3.3.1} \quad (\text{B.25})$$

$$\leq (c^4 + s^4)\frac{1}{2} + 2c^2s^2F(\rho_1) \quad \text{by Lemma 3.3.3} \quad (\text{B.26})$$

$$\leq (c^4 + s^4)\frac{1}{2} + 2c^2s^2 \quad (\text{B.27})$$

$$= \frac{1}{2}(c^4 + s^4 + 2c^2s^2) + c^2s^2 \quad (\text{B.28})$$

$$= \frac{1}{2} + c^2s^2 \quad (\text{B.29})$$

The inequality has to hold even if we maximize over the unitary operators  $\mathcal{U}_A$  and  $\mathcal{U}_B$  since the right-hand-side of this inequality is constant, whereas  $F(\rho_{\text{output}})$  allows

an arbitrary local unitary operation  $\mathcal{U}_A \otimes \mathcal{U}_B$  to be performed before taking the partial trace over one of the copies.

But the initial entanglement was

$$F(|\Psi_{\text{input}}\rangle\langle\Psi_{\text{input}}|) = |\langle\phi^+|(c|0+\rangle + s|1-\rangle)|^2 \quad (\text{B.30})$$

$$= \left| \frac{1}{\sqrt{2}}(c+s) \right|^2 \quad (\text{B.31})$$

$$= \frac{1}{2}(c^2 + s^2 + 2*cs) \quad (\text{B.32})$$

$$= \frac{1}{2} + cs. \quad (\text{B.33})$$

Thus, since  $c, s \in [0, 1]$

$$F(\rho_{\text{output}}) \leq F(|\Psi_{\text{input}}\rangle\langle\Psi_{\text{input}}|) \quad (\text{B.34})$$

with equality if and only if  $c = 0$  or  $s = 0$  (separable input state).  $\square$

# Appendix C

## Tables

38

### C.1 Entanglement Distillation Protocols

**Table C.1:** Some previously known entanglement distillation protocols. Refer to the cited articles in the column “reference” for the description and proof of correctness of these protocols. The protocols take  $n$  states of the form given in the column “input state” and produce  $m$  output states of fidelity  $\varphi_{\text{out}}$  w.r.t. a specific maximally entangled state if they succeed (with probability  $p_{\text{succ}}$ ). The protocols listed above the thin line are protocols that are applied on pure states, whereas those below that line are protocols for mixed states. Whether the protocol includes classical communication from Alice to Bob in one or both directions is shown in the column denoted as “comm.”. In the column named “prev. knowledge”, the variables that have to be known in advance, i.e. before the execution of the protocol, are listed. An approximate-equality symbol “ $\approx$ ” in the column “ $m$ ” indicates that the corresponding value is realized in the limit as  $n \rightarrow \infty$ . The four Bell states are denoted as  $|\phi_{ij}\rangle$ , where  $i, j \in \{0, 1\}$ . Note that the order of the enumeration of the Bell states causes no loss of generality, since Alice and Bob can permute the Bell states by local unitary operations[5].



$n$	$m$	input state	name of the protocol	comm.	prev. knowledge	success prob. $p_{\text{succ}}$	output fidelity $\varphi_{\text{out}}$	reference
1	1	$ \psi\rangle = c 0+\rangle + s 1-\rangle$	Procrustean (Filtering)	1-way	c,s	$2\min(c^2, s^2)$	1	[12, 38, 39]
1	1	$ \psi\rangle = \psi_{AA} \otimes \psi_{AB}$ , where $\psi_{AA} = c 00\rangle + s 11\rangle$ is the state of a pair of qubits completely in Alice's possession, whereas $\psi_{AB} = c 0+\rangle + s 1-\rangle$ belongs to a pair that is distributed to Alice and Bob.	Entanglement Swapping	1-way	none	$2c^2s^2$	1 with probability $p_{\text{succ}}$ or else $\varphi_{00} = \frac{1}{2}(1 - 2c^2 + 2c^4)^{-1}$ , $\varphi_{01} = 1 - \varphi_{00}$	[23]
$\gg 1$	$\approx nE_{\text{init}}$	$ \psi\rangle^{\otimes n} = (c 0+\rangle + s 1-\rangle)^{\otimes n}$ with entropy of entanglement $E_{\text{init}} > 0$	Schmidt Projection	no	none	1 as $n \rightarrow \infty$	1	[12, 39, 40]
1	1	$\varphi \phi^+\rangle\langle\phi^+  + (1-\varphi) 0+\rangle\langle 0+ $	Filtering	2-way	none	$\varphi\varepsilon + (1-\varphi)\varepsilon^2$	$\varphi\varepsilon/p_{\text{succ}}$	[41, 42]
2	1	$\rho_{\text{pair}} = \rho_{W,1} \otimes \rho_{W,2}$ , where $\rho_{W,1}$ and $\rho_{W,2}$ are Werner states i.e. $\rho_{W,k} = \frac{1}{3}(4\varphi_k - 1) \phi^+\rangle\langle\phi^+  + \frac{1}{3}(1 - \varphi_k)\mathbb{1}_{AB}$ with $\varphi_1, \varphi_2 > \frac{1}{2}$	BBPSSW (for recursive and nested schemes)	2-way	none	$\frac{1}{9}(5 - 2\varphi_2 + \varphi_1(8\varphi_2 - 2))$	$\frac{1}{9}(1 - \varphi_2 + \varphi_1(10\varphi_2 - 1))/p_{\text{succ}}$	[4, 5, 43, 42]
2	1	$\rho_{\text{pair}} = \rho_1 \otimes \rho_2$ , where $\rho_1$ and $\rho_2$ are Bell diagonal i.e. $\rho_k = \sum_{i,j,k} \varphi_{i,j,k}  \phi_{i,j,k}\rangle\langle\phi_{i,j,k} $ with $\varphi_{00,1}, \varphi_{00,2} > \frac{1}{2}$	DEJMPS (for recursive and nested schemes)	2-way	none	$(\varphi_{00,1} + \varphi_{11,1})(\varphi_{00,2} + \varphi_{11,2}) + (\varphi_{01,1} + \varphi_{10,1})(\varphi_{01,2} + \varphi_{10,2})$	$\varphi_{00,\text{out}} = (\varphi_{00,1}\varphi_{00,2} + \varphi_{11,1}\varphi_{11,2})/p_{\text{succ}}$ $\varphi_{01,\text{out}} = (\varphi_{01,1}\varphi_{01,2} + \varphi_{10,1}\varphi_{10,2})/p_{\text{succ}}$ $\varphi_{10,\text{out}} = (\varphi_{00,1}\varphi_{11,2} + \varphi_{11,1}\varphi_{00,2})/p_{\text{succ}}$ $\varphi_{11,\text{out}} = (\varphi_{01,1}\varphi_{10,2} + \varphi_{10,1}\varphi_{01,2})/p_{\text{succ}}$	[6, 44, 43, 42]
$\geq 2$	$< n$	any $\rho = \rho_{\text{input}}$ , where $\rho_{\text{input}} \in \mathcal{H}_{2^{2n}}$ with $\varphi(\rho_{\text{input}}) = \langle\phi^+ \rho \phi^+\rangle \geq 1 - \varepsilon$	Random Hashing	1-way	none	$\geq 1 - \varepsilon$	$1 - 2^{m-n}/(1 - \varepsilon)$	[7, 8, 45]
$\geq 2$	$< n$	any $\rho = \rho_{\text{input}} \otimes ( \phi^+\rangle\langle\phi^+ )^{\otimes k}$ , where $\rho_{\text{input}} \in \mathcal{H}_{2^{2n}}$ with $\varphi(\rho_{\text{input}}) = \langle\phi^+ \rho \phi^+\rangle \geq 1 - \varepsilon$ and $n$ and $m$ chosen such that $nk/m$ and $m/k$ are integers.	Random Permutation	2-way	none	1	$1 - \frac{2^m - 2^k}{2^m - 2^{m-1}} \varepsilon$	[7, 8, 45]
$\geq 2$	$< n$	same input as above but with a shared source of random numbers (public coin)	No-communication Random Permutation	no	none	1	$1 - \frac{3}{4} \frac{2^n - 2}{2^m - 1} \varepsilon$	[8, 45]
$\gg 1$	$\approx n(1 - S(\rho))$	$\rho^{\otimes n}$ , where $\rho$ is Bell diagonal i.e. $\rho = \sum_{i,j} \varphi_{ij}  \phi_{ij}\rangle\langle\phi_{ij} $ with von Neumann entropy $S(\rho) < 1$ combined with a number $n(S(\rho) + \delta)$ , $\delta \geq 0$ of maximally entangled states	Breeding	1-way	$\varphi_{ij}$	1 as $n \rightarrow \infty$	1	[4, 5, 42]
$\gg 1$	$\approx n(1 - S(\rho))$	$\rho^{\otimes n}$ , where $\rho$ is Bell diagonal i.e. $\rho = \sum_{i,j} \varphi_{ij}  \phi_{ij}\rangle\langle\phi_{ij} $ with von Neumann entropy $S(\rho) < 1$	Hashing	1-way	$\varphi_{ij}$	1 as $n \rightarrow \infty$	1	[5, 46, 42]

## C.2 Limits to Distillability

**Table C.2:** Some previously known limits to the existence of entanglement distillation protocols for particular input states. Refer to the cited articles for the proofs of these limits (given in the column “reference”).  $m$  denotes the number of output states which have higher fidelity  $\varphi_{\text{out}}$  than each of the  $n$  given input states. A “0” for “max.  $m$ ” means that no distillation protocol fulfilling this particular requirements exists. The limits given in the columns “max.  $m$ ” and “max.  $\varphi_{\text{out}}$ ” only apply if the requirements specified in the other columns are met. An asterisk (\*) indicates that the corresponding quantity does not matter for the limit, i.e. the limitation applies for any value of this quantity. The limits listed above the thin line are limits that apply to protocols that work on pure states, whereas those below that line are limitations on the existence of protocols for mixed states. Whether the protocol is allowed to include classical communication from Alice to Bob in one or both directions is shown in the column denoted as “comm.”. In the column named “prev. knowledge”, the variables that are given in advance, i.e. before the execution of the protocol, are listed. The column “required  $p_{\text{succ}}$ ” specifies what the desired success probability is. Note that a value of 1 means that the protocol has to be deterministic in the sense that it always has to succeed. A value of one in column “required  $\varphi_{\text{out}}$ ” means that the limitation only applies to protocols that generate maximally entangled output pairs.

$n$	$m$	input state	name of the corresponding noise model (if any)	comm.	prev. knowledge	required $p_{\text{succ}}$	required $\varphi_{\text{out}}$	max. $m$	max. $\varphi_{\text{out}}$	reference
*	*	any pure state with entropy of entanglement $E( \psi\rangle) \geq k$	Entanglement Model	*	only $k$	1	*	<b>0</b>		[45]
$\gg 1$	*	any pure state $ \psi\rangle$ with entropy of entanglement $E_{\text{init}}$		*	*	$> 0$	1	$nE_{\text{init}}$ for $n \rightarrow \infty$		[13]
*	*	any $\rho = \rho_{\text{input}} \otimes ( \phi^+\rangle\langle\phi^+ )^{\otimes k}$ , where $\rho_{\text{input}} \in \mathcal{H}_{2^{2n}}$ with $\varphi_{\text{mit}} = \varphi(\rho_{\text{input}}) \geq 1 - \varepsilon$ and $k < m$	Fidelity Model	*	only $\varepsilon$ and $k$	1	*		$1 - \frac{2^m - 2^k}{2^m} \frac{2^n}{2^n - 1} \varepsilon$	[7, 45]
*	*	same input as above but with a shared source of random numbers (public coin)	Fidelity Model	no	only $\varepsilon$ and $k$	1	*		$1 - \frac{3}{4} \frac{2^{2n}}{2^{2n} - 1} \varepsilon$	[8, 45]
*	*	$\rho = \frac{1}{2^n \binom{n}{r}} \sum_{\mathbf{v}: \text{deg}(\mathbf{v})=r}  \phi_{\mathbf{v}}\rangle\langle\phi_{\mathbf{v}} $ , where $\mathbf{v} \in \{0, 1, *\}^n$ , $\text{deg}(\mathbf{v}) :=  \{i : v_i \neq *\} $ and $ \phi_{\mathbf{v}}\rangle := \bigotimes_{j=0}^{n-1}  \phi_j\rangle$ with $ \phi_j\rangle := \begin{cases}  0+\rangle & \text{if } v_j = 0 \\  1-\rangle & \text{if } v_j = 1 \\  \phi^+\rangle & \text{if } v_j = * \end{cases}$	Bounded Measurement Model	no	*	1	*	<b>0</b>		[8, 45]
*	*	$\rho = \frac{1}{3^n \binom{n}{r}} \sum_{\mathbf{v}: \text{deg}(\mathbf{v})=r} P_{\mathbf{v}}  \langle\phi^+ \rangle^{\otimes n} P_{\mathbf{v}}^\dagger$ , $\mathbf{v} := (x_0, x_1, \dots, x_{n-1}, z_0, z_1, \dots, z_{n-1})$ , $\text{deg}(\mathbf{v}) :=  \{i : x_i \neq 0 \vee z_i \neq 0\} $ , $P_{\mathbf{v}} := X^{x_0} Z^{z_0} \otimes \dots \otimes X^{x_{n-1}} Z^{z_{n-1}}$	Bounded Corruption Model	no	*	1	*		$1 - \frac{r}{2^n}$	[45]
*	*	$\rho = (\rho_W)^{\otimes n}$ , where $\rho_p$ is a Werner state: $\rho_W = (1 - \frac{3p}{4}) \phi^+\rangle\langle\phi^+  + \frac{p}{4}( \phi^-\rangle\langle\phi^-  +  \psi^+\rangle\langle\psi^+  +  \psi^-\rangle\langle\psi^- )$	Depolarization Model	no	*	1	*		$1 - \frac{p}{2}$	[8, 45]
*	*	$\rho(p) = (\Omega_\alpha)^{\otimes n}$ , where $\Omega_\alpha = \frac{1+\alpha}{2}  \phi^+\rangle\langle\phi^+  + \frac{1-\alpha}{2}  \phi^-\rangle\langle\phi^- $	Weakly Entangled Mixed States	no	*	1	*	<b>0</b>		[14]
2	*	$\rho(p) = p\rho_0 + (1-p)\rho_1$ , $p \in [0, 1]$ , where $\rho(p) \in S$ and $S$ is a <i>twirlable</i> family of bipartite mixed states, e.g the family of all Werner states (see reference).		*	*	1	*	<b>0</b>		[15]

### C.3 Optimization Runs

In the following, tables summarizing the properties of the performed numerical optimizations are presented.

**Table C.3:** Listing of the performed optimization runs for the case of symmetric distillation with an orthogonal matrix for 3 copies of a pure input state together with 2 ancilla qubits per party (Section 5.3.1). The dimensionality of the search space was 497. The “run id” is an arbitrary identifier of the run. In the column “initial parameters”, either the distribution with which the initial parameters have been sampled is given or else the parameters were exactly the same as in a previous optimization run (“same as ...”). “resumed from ...” means that the corresponding run has been continued from of a former run. The term “param.” in the column denoted as “det.”, means that the determinant was set by the sign of an additional parameter. For an explanation of the algorithm specific parameters  $\sigma$  and  $\lambda$ , refer to Section 5.2. The value given in the column “total # f. e.” is the total number of function evaluations, whereas the value given in “needed # f. e.” is the number of function evaluations needed to reach the final fitness value given in the column “final fitness” up to an accuracy of 5 decimals. The given fitness values can be converted directly to fidelities by subtracting the fitness from 1. The fidelity of the input state was 0.8 for all runs. Thus, only those runs with fitness  $< 0.2$  were successful in finding an entanglement distillation protocol. The time the CPU used to perform the optimization is given in the column “runtime CPU”. The optimizations have been performed on a cluster which automatically distributes the jobs to specific nodes. Those nodes have different CPUs. The speed of the CPU is indicated by the so called “CPU factor”. The corresponding CPU models are: 6.5: AMD Opteron 250, 7.5: AMD Opteron 8380, 8.0: AMD Opteron 2220

run id	initial parameters	det.	init. $\sigma$	$\lambda$	total # f. e.	needed # f. e.	initial fitness	final fitness	runtime CPU	CPU factor
1	$\mathcal{N}(\mathbf{0}, (0.0814)^2)$	param.	0.01	22	233289	79729	0.45097	0.16400	n/a	n/a
2	$\mathcal{N}(\mathbf{0}, (0.0814)^2)$	param.	0.01	22	269699	87539	0.48775	0.16400	n/a	n/a
z	all zero	param.	0.01	22	299223	146191	0.20000	0.16400	n/a	n/a
3	$\mathcal{U}([-\pi, +\pi])$	param.	$2\pi/\sqrt{12}$	22	89167	28205	0.45196	0.32802	n/a	n/a
4	$\mathcal{U}([-\pi, +\pi])$	param.	0.01	22	2442287	249767	0.48753	0.20300	n/a	n/a
5	same as 4	param.	0.01	22	42571	38831	0.48753	0.20333	n/a	n/a
6	same as 4	param.	0.01	22	28601	28183	0.48753	0.20434	39min	6.5
6.1	resumed from 6	param.	-	22	300015	258171	-	0.20300	4h 06min	7.5
7	same as 4	param.	0.01	22	300015	287013	0.48753	0.20300	4h 27min	7.5
8	same as 4	param.	0.01	22	300015	286947	0.48753	0.20300	5h 19min	7.5
10	$\mathcal{U}([-\pi, +\pi])$	+1	0.01	22	300015	239053	0.44144	0.20300	6h 52min	6.5
11	same as 10	+1	0.01	22	300015	260503	0.44144	0.20300	6h 49min	6.5
12	same as 10	-1	0.01	22	300015	223081	0.44144	0.20300	7h 13min	6.5

table continued on next page

run id	initial parameters	det.	init. $\sigma$	$\lambda$	total # f. e.	needed # f. e.	initial fitness	final fitness	runtime CPU	CPU factor
13	same as 10	-1	0.01	22	300015	231947	0.44144	0.20300	6h 48min	6.5
15	$\mathcal{U}([- \pi, + \pi])$	+1	0.01	22	300015	220221	0.41733	0.20300	7h 02min	6.5
16	$\mathcal{U}([- \pi, + \pi])$	+1	0.01	22	300015	235027	0.46305	0.20300	6h 49min	6.5
17	$\mathcal{U}([- \pi, + \pi])$	-1	0.01	22	300015	254783	0.43582	0.20000	7h 20min	6.5
18	$\mathcal{U}([- \pi, + \pi])$	param.	0.01	22	300015	251021	0.44511	0.20300	5h 31min	8.0
18.1	resumed from 18	param.	-	22	600007	251021	-	0.20300	5h 45min	8.0
19	$\mathcal{U}([- \pi, + \pi])$	param.	0.01	22	6403	6007	0.50830	0.20735	9min	6.5
19.1	resumed from 19	param.	-	22	1000011	257709	-	0.20000	18h 19min	8.0
20	$\mathcal{U}([- \pi, + \pi])$	param.	0.01	22	300015	256807	0.46339	0.20300	6h 59min	6.5

**Table C.4:** Listing of the performed optimization runs for the case of general entanglement distillation for 3 copies of a pure input state together with 2 ancilla qubits per party (Section 5.3.2). The dimensionality of the search space was 2048. The “run id” is an arbitrary identifier of the run. In column “initial parameters”, either the distribution with which the initial parameters have been sampled is given or else the parameters were exactly the same as in a previous optimization run (“same as ...”) or the corresponding run is a continuation of a former run (“resumed from ...”). For an explanation of the algorithm specific parameters  $\sigma$  and  $\lambda$ , refer to Section 5.2. The value given in the column “total # f. e.” is the total number of function evaluations, whereas the value given in “needed # f. e.” is the number of function evaluations needed to reach the final fitness value given in the column “final fitness” up to an accuracy of 5 decimals. The given fitness values can be converted directly to fidelities by subtracting the fitness from 1. The fidelity of the input state was 0.8 for all runs. Thus, only those runs with fitness  $< 0.2$  were successful in finding an entanglement distillation protocol within the limited number of function evaluations. The time the CPU used to perform the optimization is given in the column “runtime CPU”. The optimizations have been performed on a cluster which automatically distributes the jobs to specific nodes. Those nodes have different CPUs. The speed of the CPU is indicated by the so called “CPU factor”. The corresponding CPU models are: 6.5: AMD Opteron 250, 7.5: AMD Opteron 8380, 8.0: AMD Opteron 2220

run id	initial parameters	init. $\sigma$	$\lambda$	total # f. e.	needed # f. e.	initial fitness	final fitness	runtime CPU	CPU factor
1	$\mathcal{U}([-\pi, \pi])$	0.01	26	44773	44461	0.73277	0.17946	11h 33min	6.5
2	same as 1	0.01	26	100023	99867	0.73277	0.17532	17h 56min	6.5
3	same as 1	0.01	26	95083	92587	0.73277	0.17578	n/a	n/a
8	same as 1	0.01	26	100023	100023	0.73277	0.17511	8h 08min	8.0
8.1	resumed from 8	-	26	300015	291490	-	0.16842	20h 53min	6.5
8.2	resumed from 8.1	-	26	600003	593867	-	0.16728	23h 57min	8.0
9	same as 1	0.01	26	100023	99815	0.73277	0.17534	10h 14min	6.5
9.1	resumed from 9	-	26	300015	297181	-	0.16825	20h 39min	6.5
15	$\mathcal{U}([-\pi, \pi])$	0.01	26	200019	196919	0.71485	0.20524	16h 53min	8.0
15.1	resumed from 15	-	26	600003	591033	-	0.20296	32h 20min	8.0
16	$\mathcal{U}([-\pi, \pi])$	0.01	26	200019	199161	0.71485	0.20520	16h 40min	8.0
16.1	resumed from 16	-	26	600003	590487	-	0.20036	32h 45min	8.0
17	$\mathcal{U}([-\pi, \pi])$	0.01	26	200019	195833	0.67071	0.17284	16h 05min	8.0

**Table C.5:** Listing of the performed optimization runs for the case of entanglement distillation for 2 copies of a pure input state together with 2 ancilla qubits per party (Section 5.4). The “run id” is an arbitrary identifier of the run. In the column “initial parameters”, either the distribution with which the initial parameters have been sampled is given or else the parameters were exactly the same as in a previous optimization run (“same as ...”) or the corresponding run has been continued from a former run (“resumed from ...”). The dimensionality of the search space depends on the restrictions that have been applied. If the value in the column “sym.” is true, then the unitary matrices  $\mathbf{U}_A$  and  $\mathbf{U}_B$  were restricted to be the same. If the column “orth.” contains a true, then  $\mathbf{U}_A$  and  $\mathbf{U}_B$  were restricted to be orthogonal matrices. In the case of orthogonal matrices, the sign of the determinant is either set by a parameter which is indicated by the term “param” in the column denoted as “det.”. Otherwise, the column “det.” contains the value to which the determinant was set. For an explanation of the algorithm specific parameters  $\sigma$  and  $\lambda$ , refer to Section 5.2. The value given in the column “total # f. e.” is the total number of function evaluations, whereas the value given in “needed # f. e.” is the number of function evaluations needed to reach the final fitness value given in the column “final fitness” up to an accuracy of 5 decimals. The given fitness values can be converted directly to fidelities by subtracting the fitness from 1. The fidelity of the input state was 0.8 for all runs. Thus, only those runs with fitness  $< 0.2$  were successful in finding an entanglement distillation protocol within the limited number of function evaluations. The time the CPU used to perform the optimization is given in “runtime CPU”. The optimizations have been performed on a cluster which automatically distributes the jobs to specific nodes. Those nodes have different CPUs. The speed of the CPU is indicated by the so called “CPU factor”. The corresponding CPU models are: 6.5: AMD Opteron 250, 7.5: AMD Opteron 8380, 8.0: AMD Opteron 2220

run id	initial param.	sym.	orth.	det.	init. $\sigma$	$\lambda$	total # f. e.	needed # f. e.	initial fitness	final fitness	runtime CPU	CPU factor
sr1	$\mathcal{U}([- \pi, \pi])$	true	true	1	0.1	18	226063	51913	0.50584	0.20000	0h 25min	8.0
sr2	$\mathcal{U}([- \pi, \pi])$	true	true	-1	0.1	18	164665	23779	0.50472	0.20000	0h 19min	8.0
sr3	all zero	true	true	-1	0.1	18	41113	0	0.20000	0.20000	0h 05min	7.5
sr4	all zero	true	true	1	0.1	18	41419	0	0.20000	0.20000	0h 05min	8.0
r1	all zero	false	true	param.	0.1	20	125601	0	0.20000	0.20000	0h 19min	7.5
r2	all zero	false	true	param.	0.1	20	232441	0	0.20000	0.20000	0h 38min	7.5
r3	$\mathcal{U}([- \pi, \pi])$	false	true	1	0.1	20	748661	13421	0.55897	0.20000	1h 02min	8.0
r4	$\mathcal{U}([- \pi, \pi])$	false	true	1	0.1	20	583841	4978	0.51957	0.23000	1h 35min	8.0
g1	$\mathcal{U}([- \pi, \pi])$	false	false	-	0.1	22	300015	283845	0.77006	0.20001	1h 40min	8.0
g1.2	resumed from g1	false	false	-	-	22	1000011	15750	-	0.20000	4h 18min	8.0
g2	$\mathcal{U}([- \pi, \pi])$	false	false	-	0.1	22	300015	197935	0.77387	0.20000	1h 36min	7.5
g2.2	resumed from g2	false	false	-	-	22	567909	197935	-	0.20000	1h 51min	8.0

**Table C.6:** Listing of the performed optimization runs for the case of entanglement distillation for 3 copies of a Werner state (5.10) together with 2 ancilla qubits per party (Section 5.5). The “run id” is an arbitrary identifier of the run. In the column “initial parameters”, either the distribution with which the initial parameters have been sampled is given or else the parameters were exactly the same as in a previous optimization run (“same as ...”) or the corresponding run is a continuation of a former run (“resumed from ...”). The dimensionality of the search space depends on the restrictions that have been applied. If the value in the column “sym.” is true, then the unitary matrices  $\mathbf{U}_A$  and  $\mathbf{U}_B$  were restricted to be the same. If the column “orth.” contains a true, then  $\mathbf{U}_A$  and  $\mathbf{U}_B$  were restricted to be orthogonal matrices. In the case of orthogonal matrices, the sign of the determinant is either set by a parameter which is indicated by the term “param” in the column denoted as “det.”. Otherwise, the column “det.” contains the value to which the determinant was set. For an explanation of the algorithm specific parameters  $\sigma$  and  $\lambda$ , refer to Section 5.2. The value given in the column “total # f. e.” is the total number of function evaluations, whereas the value given in “needed # f. e.” is the number of function evaluations needed to reach the final fitness value given in the column “final fitness” up to an accuracy of 5 decimals. The given fitness values can be converted directly to fidelities by subtracting the fitness from 1. The fidelity of the input state was 0.925 for all runs. Thus, only those runs with fitness smaller than 0.075 were successful in finding an entanglement distillation protocol within the limited number of function evaluations. The time the CPU used to perform the optimization is given in “runtime CPU”. The optimizations have been performed on a cluster which automatically distributes the jobs to specific nodes. Those nodes have different CPUs. The speed of the CPU is indicated by the so called “CPU factor”. The corresponding CPU models are: 6.5: AMD Opteron 250, 7.5: AMD Opteron 8380, 8.0: AMD Opteron 2220

run id	initial param.	sym.	orth.	det.	init. $\sigma$	$\lambda$	total # f. e.	needed # f. e.	initial fitness	final fitness	runtime CPU	CPU factor
sr1	$\mathcal{U}([-\pi, \pi])$	true	true	param.	0.01	22	91983	91631	0.50373	0.12013	34h 20min	6.5
sr2	same as 1	true	true	param.	0.01	22	91983	91125	0.50373	0.12009	34h 05min	6.5
sr3	all zero	true	true	+1	0.01	22	100013	1	0.07500	0.07500	18h 34min	8.0
sr4	all zero	true	true	+1	0.01	22	100013	1	0.07500	0.07500	18h 20min	8.0
sr5	all zero	true	true	-1	0.01	22	100013	1	0.11888	0.11888	18h 34min	8.0
sr6	all zero	true	true	-1	0.01	22	100013	1	0.11888	0.11888	18h 28min	8.0
s1	$\mathcal{U}([-\pi, \pi])$	true	false	-	0.01	24	12577	12565	0.71130	0.37129	28h 33min	8.0
s1.1	resumed from s1	true	false	-	-	24	47665	46199	-	0.17446	34h 48min	8.0
s2	$\mathcal{U}([-\pi, \pi])$	true	false	-	0.01	24	51721	51516	0.67241	0.13511	34h 38min	8.0
g1	$\mathcal{U}([-\pi, \pi])$	false	false	-	0.01	26	8009	7984	0.74997	0.53858	24h 20min	6.5
g2	same as g1	false	false	-	0.01	26	8009	7984	0.74997	0.54449	18h 44min	8.0



# Bibliography

- [1] J. S. Bell. “On the Einstein-Podolsky-Rosen paradox”. In: *Physics* 1.3 (1964), pp. 195–200.
- [2] C. H. Bennett et al. “Teleporting an unknown quantum state via dual classical and Einstein-Podolsky-Rosen channels”. In: *Phys. Rev. Lett.* 70.13 (Mar. 1993), pp. 1895–1899. DOI: 10.1103/PhysRevLett.70.1895.
- [3] C. H. Bennett and S. J. Wiesner. “Communication via one- and two-particle operators on Einstein-Podolsky-Rosen states”. In: *Phys. Rev. Lett.* 69.20 (Nov. 1992), pp. 2881–2884. DOI: 10.1103/PhysRevLett.69.2881.
- [4] C. H. Bennett et al. “Purification of Noisy Entanglement and Faithful Teleportation via Noisy Channels”. In: *Phys. Rev. Lett.* 76.5 (Jan. 1996), pp. 722–725. DOI: 10.1103/PhysRevLett.76.722.
- [5] C. H. Bennett et al. “Mixed-state entanglement and quantum error correction”. In: *Phys. Rev. A* 54.5 (Nov. 1996), pp. 3824–3851. DOI: 10.1103/PhysRevA.54.3824.
- [6] D. Deutsch et al. “Quantum Privacy Amplification and the Security of Quantum Cryptography over Noisy Channels”. In: *Phys. Rev. Lett.* 77.13 (Sept. 1996), pp. 2818–2821. DOI: 10.1103/PhysRevLett.77.2818.
- [7] A. Ambainis, A. Smith, and K. Yang. “Extracting quantum entanglement (general entanglement purification protocols)”. In: *Computational Complexity, 2002. Proceedings. 17th IEEE Annual Conference on.* 2002, pp. 82–91. DOI: 10.1109/CCC.2002.1004345.
- [8] A. Ambainis and K. Yang. “Towards the classical communication complexity of entanglement distillation protocols with incomplete information”. In: *Computational Complexity, 2004. Proceedings. 19th IEEE Annual Conference on.* June 2004, pp. 305–319. DOI: 10.1109/CCC.2004.1313853.
- [9] N. Hansen and A. Ostermeier. “Completely Derandomized Self-Adaptation in Evolution Strategies”. In: *Evol. Comput.* 9.2 (2001), pp. 159–195. ISSN: 1063-6560. DOI: 10.1162/106365601750190398.
- [10] A. Einstein, B. Podolsky, and N. Rosen. “Can Quantum-Mechanical Description of Physical Reality Be Considered Complete?” In: *Physical Review Online Archive (Prola)* 47.10 (May 1935), pp. 777–780. DOI: 10.1103/PhysRev.47.777.
- [11] C. H. Bennet and G. Brassard. “Quantum Cryptography: Public Key Distribution and Coin Tossing”. In: *International Conference on Computers, Systems & Signal Processing Bangalore, India.* 1984.
- [12] C. H. Bennett et al. “Concentrating partial entanglement by local operations”. In: *Phys. Rev. A* 53.4 (Apr. 1996), pp. 2046–2052. DOI: 10.1103/PhysRevA.53.2046.

- [13] H.-K. Lo and S. Popescu. “Concentrating entanglement by local actions: Beyond mean values”. In: *Phys. Rev. A* 63.2 (Jan. 2001), p. 022301. DOI: 10.1103/PhysRevA.63.022301.
- [14] D. D. Dukaric and S. Wolf. “A Limit on Non-Locality Distillation”. In: *arXiv eprints* (Aug. 2008). arXiv:quant-ph/0808.3317.
- [15] A. J. Short. “No Deterministic Purification for Two Copies of a Noisy Entangled State”. In: *Phys. Rev. Lett.* 102.18 (May 2009), p. 180502. DOI: 10.1103/PhysRevLett.102.180502.
- [16] A. Messiah. *Quantum Mechanics, Two Volumes Bound as One*. Dover Publications Inc., Mineola, New York, 1999.
- [17] C. Cohen-Tannoudji, B. Diu, and F. Laloe. *Quantum Mechanics (2 vol. set)*. Wiley-Interscience, Oct. 2006. ISBN: 0471569526.
- [18] M. A. Nielsen and I. L. Chuang. *Quantum Computation and Quantum Information*. 1st ed. Cambridge University Press, Oct. 2000. ISBN: 0521635039.
- [19] P. J. Mohr, B. N. Taylor, and D. B. Newell. “CODATA recommended values of the fundamental physical constants: 2006”. In: *Reviews of Modern Physics* 80.2, 633 (2008), p. 633. DOI: 10.1103/RevModPhys.80.633.
- [20] A. Aspect, J. Dalibard, and G. Roger. “Experimental Test of Bell’s Inequalities Using Time-Varying Analyzers”. In: *Phys. Rev. Lett.* 49.25 (Dec. 1982), pp. 1804–1807. DOI: 10.1103/PhysRevLett.49.1804.
- [21] J. Grondalski, D. M. Etlinger, and D. F. V. James. “The fully entangled fraction as an inclusive measure of entanglement applications”. In: *Physics Letters A* 300.6 (2002), pp. 573–580. ISSN: 0375-9601. DOI: 10.1016/S0375-9601(02)00884-8.
- [22] M.-J. Zhao and Z.-X. W. Zong-Guo Li Shao-Ming Fei. “A Note on Fully Entangled Fraction”. In: *arXiv eprints* (June 2010). arXiv:1006.3502v2.
- [23] S. Bose, V. Vedral, and P. L. Knight. “Purification via entanglement swapping and conserved entanglement”. In: *Phys. Rev. A* 60.1 (July 1999), pp. 194–197. DOI: 10.1103/PhysRevA.60.194.
- [24] M. A. Nielsen. “Conditions for a Class of Entanglement Transformations”. In: *Phys. Rev. Lett.* 83.2 (July 1999), pp. 436–439. DOI: 10.1103/PhysRevLett.83.436.
- [25] A. Mordecai. *Nonlinear Programming: Analysis and Methods*. Dover Publishing, Oct. 2003. ISBN: 0-486-43227-0.
- [26] J. B. Lasserre. “Global Optimization with Polynomials and the Problem of Moments”. In: *SIAM Journal on Optimization* 11.3 (2001), pp. 796–817. DOI: 10.1137/S1052623400366802.
- [27] H. Waki et al. “Sums of Squares and Semidefinite Program Relaxations for Polynomial Optimization Problems with Structured Sparsity”. In: *SIAM Journal on Optimization* 17.1 (2006), pp. 218–242. DOI: 10.1137/050623802.
- [28] H. Waki et al. “Algorithm 883: SparsePOP—A Sparse Semidefinite Programming Relaxation of Polynomial Optimization Problems”. In: *ACM Trans. Math. Softw.* 35 (2 July 2008), 15:1–15:13. ISSN: 0098-3500. DOI: 10.1145/1377612.1377619.
- [29] K. Fujii, K. Funahashi, and T. Kobayashi. “Jarlskog’s Parametrization of Unitary Matrices and Qudit Theory”. In: *ArXiv Quantum Physics e-prints* (July 2005). arXiv:quant-ph/0508006.

- [30] C. Jarlskog. “Recursive parametrization and invariant phases of unitary matrices”. In: *Journal of Mathematical Physics* 47.1, 013507 (2006), p. 013507. DOI: 10.1063/1.2159069.
- [31] R. C. Raffinetti and K. Ruedenberg. “Parametrization of an orthogonal matrix in terms of generalized eulerian angles”. In: *International Journal of Quantum Chemistry* 4.S3B (1969), pp. 625–634. ISSN: 1097-461X. DOI: 10.1002/qua.560040725.
- [32] D. K. Hoffman, R. C. Raffinetti, and K. Ruedenberg. “Generalization of Euler Angles to N-Dimensional Orthogonal Matrices”. In: *Journal of Mathematical Physics* 13.4 (1972), pp. 528–533. DOI: 10.1063/1.1666011.
- [33] N. Hansen. “The CMA Evolution Strategy: a comparing review”. In: *Towards a new evolutionary computation. Advances on estimation of distribution algorithms*. Ed. by J. Lozano et al. Springer, 2006, pp. 75–102.
- [34] I. Rechenberg. *Evolutionsstrategie: Optimierung technischer Systeme nach Prinzipien der biologischen Evolution*. Stuttgart: Fromman-Holzboog, 1973.
- [35] H.-P. Schwefel. “Evolutionsstrategie und numerische Optimierung”. Dr.-Ing. Dissertation. Technische Universität Berlin, Fachbereich Verfahrenstechnik, 1975.
- [36] N. Hansen, S. Muller, and P. Koumoutsakos. “Reducing the time complexity of the derandomized Evolution Strategy with covariance matrix adaptation (CMA-ES)”. In: *Evolutionary Computation* 11.1 (2003), pp. 1–18.
- [37] V. Strassen. “Gaussian elimination is not optimal”. In: *Numerische Mathematik* 13 (4 1969). 10.1007/BF02165411, pp. 354–356. ISSN: 0029-599X.
- [38] P. G. Kwiat et al. “Experimental entanglement distillation and ‘hidden’ non-locality”. In: *Nature* 409.6823 (2001), pp. 1014–1017. DOI: 10.1038/35059017.
- [39] S. Popescu and D. Rohrlich. “The joy of entanglement”. In: *Introduction to Quantum Computation*. Ed. by H.-K. Lo, S. Popescu, and T. P. Spiller. Singapore: World-Scientific, 1998, pp. 29–48.
- [40] J. Preskill. *Lecture Notes for Physics 229: Quantum Information and Computation*.
- [41] N. Gisin. “Hidden quantum nonlocality revealed by local filters”. In: *Physics Letters A* 210.3 (1996), pp. 151–156. ISSN: 0375-9601. DOI: 10.1016/S0375-9601(96)80001-6.
- [42] W. Dür and H.-J. Briegel. “Purification and Distillation”. In: *Lectures on Quantum Information*. Ed. by D. Bruß and G. Leuchs. Wiley-VCH, 2007, pp. 177–208. ISBN: 3527405275.
- [43] W. Dür and H.-J. Briegel. “Entanglement Purification for Quantum Computation”. In: *Phys. Rev. Lett.* 90.6 (Feb. 2003), p. 067901. DOI: 10.1103/PhysRevLett.90.067901.
- [44] C. Macchiavello. “On the analytical convergence of the QPA procedure”. In: *Physics Letters A* 246.5 (1998), pp. 385–388. ISSN: 0375-9601. DOI: 10.1016/S0375-9601(98)00550-7.
- [45] K. Yang. “On the communication complexity of correlation and entanglement distillation”. AAI3126935. PhD thesis. Pittsburgh, PA, USA, 2004.
- [46] H. Aschauer. “Quantum communication in noisy environments”. PhD thesis. Ludwig Maximilians Universität München, 2004.